NATIONAL ADVISORY COMMITTEE FOR AERONAUTICS

TECHNICAL NOTE 2885

SOME EXACT SOLUTIONS OF TWO-DIMENSIONAL FLOWS OF COMPRESSIBLE FLUID WITH HODOGRAPH METHOD

By Chieh-Chien Chang and Vivian O'Brien

The Johns Hopkins University

Washington
February 1953

NATIONAL ADVISORY COMMITTEE FOR AERONAUTICS

TECHNICAL NOTE 2885

SOME EXACT SOLUTIONS OF TWO-DIMENSIONAL FLOWS OF COMPRESSIBLE FLUID WITH HODOGRAPH METHOD

By Chieh-Chien Chang and Vivian O'Brien

SUMMARY

A suggestion is given for classifying the compressible potential flows according to the location and number of singularities in the subsonic region of the hodograph plane, which seems to offer a convenient criterion for systematic investigation of these flows with Chaplygin's original method. The primary object of the paper is to present and analyze a few useful solutions of compressible potential flow with the exact gas law. These solutions include flows about convex corners which are the same type given by Kraft and Dibble. These flows belong to the same class as that of Ringleb, that is, they have a hodograph singularity at the origin. For this reason they are called generalized Ringleb flows. Furthermore, the exact solution of compressible flow through a particular contracting channel is given. This flow is characterized in the hodograph by a source corresponding to incoming velocity and a sink corresponding to throat velocity. The channel flow near the point of inflection of the boundary is given in detail.

INTRODUCTION

The hodograph method as applied to the two-dimensional potential flow of compressible perfect fluid was demonstrated by Molenbroek (reference 1) in 1890 and by Chaplygin (reference 2) in 1904, and has lately been formulated more extensively by Tsien and Kuo (reference 3), Lighthill (reference 4), Cherry (reference 5), Chang (reference 6), and so forth. Although the mathematical theory of the method is well established, very few exact solutions of physically interesting flows have been found. Solutions have been found by Kármán and Tsien (e.g., reference 7) and Guderley and Yoshihara (reference 8) using hypothetical gas laws. There is danger that important physical features may be lost in such approximate solutions even though the analysis is often very much simplified. It would seem worth while to obtain as many compressible flows as possible with the exact gas law.

There are a number of difficulties which impede the investigators in the search for exact solutions for compressible flow. In general, there are singularities in the flow field which make analytic continuation necessary. The analytic continuation even across a simple pole is complicated for compressible flow. It would be a formidable mathematical task to find the analytic continuation across the higher-order singularities. Lighthill's (reference 4) or Cherry's (reference 5) method of expressing Chaplygin's function of complex eigenvalue in terms of a series of Chaplygin's functions of positive integral values sounds fine analytically; however, in practice the numerical calculation is rather impractical.

Huckel's tables (reference 9) are the only satisfactory ones on the Chaplygin function (which is, in effect, a variety of hypergeometric functions of the Mach number depending on two parameters, i.e., the specific heat ratio γ and the eigenvalue n) covering a large enough range of n with small enough intervals of Mach number M to determine the necessary information for a compressible flow of the perfect gas with $\gamma = 1.4$. Even with Huckel's tables, the range and intervals of Mach number and of eigenvalue n are too limited for calculating the flow in many cases. The series solution representing the stream function in the hodograph plane converges very slowly near flow singularities, if they are not at the origin. Many more terms (corresponding to larger values of n) than those available in the tables are needed in order to obtain a closer estimation to flow behavior. Also the existing methods of summing a slowly converging series are rather inadequate to handle the present problem. The unpublished method of Shanks[1] (reference 10) for summing such series seems a step forward, and it was certainly helpful for the present work.

For very large values of n, the asymptotic solutions of the Chaplygin function in the sense of Cherry (reference 11) require tables of Bessel functions of both the first and second kind. Although many Bessel functions have been calculated by the Harvard Computation Laboratory, National Bureau of Standards, and others, the tabulation of Bessel functions of the second kind is quite incomplete.

To avoid the above difficulties, the authors attempt to show with the hodograph method a few simple solutions of compressible flow which require no analytic continuation and are just within the capacity of a desk computer and the range of existing tables. It is well-known that the simple Ringleb solution (reference 12) on the curved convergent-divergent nozzle shows many interesting properties of smooth transonic potential flow. In principle, this compressible Ringleb flow is deduced from the incompressible flow turning around a semi-infinite thin plate. This corresponds to a doublet at the hodograph origin.

---

[1]The authors are indebted to Dr. G. S. S. Ludford for obtaining a copy of Shanks' paper.

Kraft and Dibble (reference 13) have studied a more general class of hodograph flows with a multiple pole at the origin and boundaries composed of constant θ and constant velocity magnitude q. Each flow then covers a sector of a circle about the origin in the hodograph plane. The Ringleb flow is a special case of this class of flows, as are the generalized Ringleb flows to be discussed later. Among others, Kraft and Dibble give the detailed smooth flow pattern for flow turning about a 60° corner angle which is obtained numerically with the differential analyzer. The solid boundary is composed of straight lines and a rounded corner, where the velocity magnitude is constant everywhere on the corner.

Corresponding to multiple-order singularities at the origin, a family of compressible flows are derived here from the incompressible flow about a sharp convex corner. Such an approach had been briefly indicated in reference 14. These flows belong to the class of Ringleb flows and are therefore called generalized Ringleb flows. Although much had been learned from the original Ringleb flow and the flows of Kraft and Dibble, there still remained some unexplored features that such a family of flows might illuminate:

(1) The effect of the size of the corner angle upon the maximum possible velocity for smooth isentropic flow

(2) The nature and influence of the limiting line for different members of this flow family

(3) The identification of all the pieces of hodograph flow with the flow in the physical plane

The present treatment attempts to cover this unknown ground with the simple calculating tools available to an ordinary researcher. There are still a number of things which call for further investigation.

Another interesting example is the compressible flow through a two-dimensional contraction channel. The imposed conditions on the flow are: (a) The low-velocity incoming flow is uniform and parallel to the x-axis and (b) the outgoing flow is uniform, parallel to the axis, and of higher speed. So far, no exact solution for such a compressible channel flow is available. In order to show the essential features without becoming involved in too complicated an analysis, the ratio of incoming to outgoing velocity in the channel flow of the incompressible fluid (reference 15) is assumed equal to 1/2, (i.e., ratio of inlet area and throat area is 2:1) without specifying the geometry of the channel. The domain of flow in the hodograph is restricted to lie within the annular region between the hodograph source corresponding to the incoming flow and the hodograph sink corresponding to the outgoing flow. Consequently, the entire flow in the hodograph can be represented by a single series without the complication of analytic continuation. There is, however, a disadvantage due to this choice; namely, the channel becomes infinitely long. In consequence it is difficult to calculate the whole flow field numerically and so only the channel boundary is given and the channel flow in the neighborhood of the point of inflection is shown in detail.

An amplification of Huckel's tables was made for the present calculation and is included in the report as tables 1 to 4. These tables were calculated with the ordinary desk computer and are expected to be accurate to the third place. (See appendix A.)

This paper offers a simple means of classifying potential compressible flow according to the location and number of the hodograph singularities in the subsonic domain instead of the singularities in the physical plane. Examples are given for each group, some well-known, some new. The flows are restricted to only those which can be treated with Chaplygin's method (reference 2). Perhaps such a classification will lead to systematic investigation of useful solutions of hodograph equations in the future.

The authors wish to express their appreciation to Professor F. H. Clauser for giving constructive criticism to this project and also to Mr. B. T. Chu for his valuable assistance. This investigation was carried out in the Aeronautics Department, The Johns Hopkins University, under the sponsorship and with the financial assistance of the National Advisory Committee for Aeronautics.

CLASSIFICATION OF TYPES OF FLOWS

ACCORDING TO HODOGRAPH SINGULARITIES

The laws of mass and momentum conservation of the isentropic, irrotational flow of an inviscid, compressible fluid can be expressed in terms of a single differential equation (reference 3):

$$\left(a^2 - u^2\right)\psi_{xx} - 2uv\psi_{xy} + \left(a^2 - v^2\right)\psi_{yy} = 0 \tag{1}$$

where x and y are rectangular coordinates, u and v are the respective velocity components, a is the local sound velocity, and ψ is the stream function defined by

$$\left.\begin{aligned} u &= \frac{\rho_o}{\rho}\psi_y \\ v &= -\frac{\rho_o}{\rho}\psi_x \end{aligned}\right\} \tag{2}$$

Here ρ is the local density and the subscript o refers to the stagnation condition. (A list of symbols is given in appendix B.)

Introduce the velocity magnitude $q = \sqrt{u^2 + v^2}$ and the constant ultimate velocity $q_m = a_o\sqrt{\frac{2}{\gamma - 1}}$. It can be shown that both a and ρ are unique functions of velocity magnitude q:

$$\left.\begin{aligned} \frac{a^2}{{a_o}^2} &= 1 - \frac{q^2}{{q_m}^2} = 1 - \tau \\ \frac{\rho}{\rho_o} &= (1 - \tau)^\beta \end{aligned}\right\} \tag{3}$$

where $\tau = q^2/{q_m}^2$ $(0 \leqq \tau \leqq 1)$ and $\beta = 1/(\gamma - 1)$.

For given boundary conditions, equation (1), being nonlinear, is very difficult to solve. Chaplygin (reference 2) presumably saw that the coefficients of the high-order derivatives of ψ contain only functions of u and v which are in turn related to the first derivatives of ψ. Consequently, he succeeds in the use of q and θ as independent variables to express the equation in the hodograph plane as

$$q^2\psi_{qq} + \left(M^2 + 1\right)q\psi_q + \left(1 - M^2\right)\psi_{\theta\theta} = 0 \tag{4}$$

where $M = q/a$ is the Mach number, being a function of q but independent of θ. The important gain of the equation in this form is its linearity, the separability of variables, and the feasible superposition of particular solutions. It is elliptic in character if $M < 1$ and hyperbolic if $M > 1$. The particular solution chosen by Chaplygin is

$$\psi(q,\theta) = \psi_n(q)e^{in\theta} \tag{5}$$

where n is real. Then $\psi_n(q)$ satisfies an ordinary differential equation where prime means differentiation with respect to q:

$$q^2\psi_n'' + \left(1 + M^2\right)q\psi_n' - n^2\left(1 - M^2\right)\psi_n = 0 \tag{6}$$

whose solution is

$$\psi_n(q) = q^n F\left(a_n,b_n;\ c_n;\ \frac{q^2}{{q_m}^2}\right) \tag{7}$$

where

$$\left.\begin{aligned} a_n + b_n &= n - \beta \\ a_n b_n &= -\frac{n(n + 1)}{2}\beta \\ c_n &= n + 1 \end{aligned}\right\} \tag{8}$$

and

$$F\left(a_n,b_n;\ c_n;\ \frac{q^2}{{q_m}^2}\right) \tag{9}$$

is a hypergeometric function. Since $F\left(a_n,b_n;\ c_n;\ \frac{q^2}{{q_m}^2}\right)$ depends only on n and γ instead of three parameters, it may be called the Chaplygin function. For $M = 0$, the incompressible case, $F = 1$ and

$\psi(q,\theta) = q^n e^{in\theta}$. Note that $e^{in\theta}$ remains the same for compressible and incompressible flow. This means that, for this particular solution, compressibility has no influence on the velocity phase angle θ. For each particular value of γ and n, the compressibility influences only the velocity magnitude, that is,

$$q^n \longrightarrow q^n F\left(a_n,b_n;\ c_n;\ \frac{q^2}{q_m^{\ 2}}\right) \tag{10}$$

This point leads Chaplygin to his famous method: If the flow or stream function of the incompressible fluid is known in the hodograph plane and is expressible in a power series of q, a corresponding compressible flow in the hodograph plane can be obtained by replacing q^n in each term of the power series by $q^n F\left(a_n,b_n;\ c_n;\ \frac{q^2}{q_m^{\ 2}}\right)$. It should be noted that there is a marked difference in the valid domain of the compressible and incompressible hodograph planes. The incompressible hodograph domain is infinite in extent while the compressible hodograph domain is restricted within the circle of ultimate velocity q_m. If the two streamlines for the same value of ψ in the compressible flow are compared, the two streamlines are not the same geometrical shape. The larger the Mach number, the more the distortion.

Chaplygin (reference 2) shows that this hodograph flow can be uniquely mapped to the physical plane as long as the flow is nowhere supersonic. Later investigators show that as long as the Jacobian $\partial(x,y)/\partial(q,\theta)$ is not singular, the hodograph flow can always be mapped conformally back to the physical plane. The boundary line where $\partial(x,y)/\partial(q,\theta) = 0$ is called the limiting line by Tollmien (reference 16) and Tsien (reference 17). Thus, in the compressible flow, the valid hodograph domain is further restricted by the limiting line, which lies inside the circle of ultimate velocity q_m in the supersonic region. Only the hodograph flow within the limiting line can be meaningful flow in the physical plane. However, if only isentropic flow is of interest, the hodograph flow should be further confined to the region within the streamline first touched by the limiting line.

There is one complicated feature with this method, that is, if the incompressible hodograph flow has one or more regular singularities in the flow region, one power series is required for each annular region of convergence between the singularities. Of course, the analytic continuation is required across the singularities. However, in applying the compressibility effect with the hypergeometric functions, the corresponding analytic continuation is very difficult to find. Cherry (reference 5) and Lighthill (reference 4) have contributed a great deal on this point for flows without circulation. As far as flows with circulation are concerned, that problem is far from being solved.

So far, the boundary conditions of equation (1) have not been discussed. The situation cannot be handled for general physical boundary conditions or even for general hodograph boundary conditions. Chaplygin's method of particular solution can treat only the simplest hodograph boundary conditions; that is, where the boundaries are composed of lines of constant θ and circular arcs of constant q, such as the flow through an aperture with inclined straight walls as shown in reference 6. Consequently, the flows can be classified only by means of the hodograph singularities. According to the order of simplicity of solution, the flow solutions are classified into the following categories:

(1) One singularity located at hodograph origin.

The simplest singularity of this type is a source at the hodograph origin, the stream function of which is $\psi = -\theta$ as shown in figure 1(a) for the incompressible flow. The streamlines are straight radial lines extending from the origin to infinity. It is interesting that this hodograph source corresponds to a physical sink which has streamlines coming from infinity and running radially into the origin. However, for the compressible flow with hodograph source at the origin (fig. 1(b)) the streamlines are tangent to the characteristics at the sonic line. The sonic circle is the limiting line and the flow cannot continue beyond this circle in the hodograph. In the physical plane, it is impossible to continue the flow inside the sonic circle.

Figures 2(a) and 2(b) show the vortex both for the incompressible flow and the compressible flow in the hodograph and physical planes. Note that a vortex in the hodograph becomes a vortex also in the physical plane. Both vortices have the same sense, and the flow near the hodograph origin corresponds to the physical flow far away and vice versa. Although the incompressible flow extends to infinity in both the hodograph and physical planes, the compressible flow is restricted within the circle of ultimate velocity q_m in the hodograph plane and outside the ultimate velocity circle in the physical plane. This is due to the fact that the ultimate-velocity circle is a streamline which is tangent to all the characteristics and is thus the limiting line.

These simple flows are well-known. They give a clear demonstration of the principles involved.

A combination of hodograph source and vortex at the origin will have the limiting line occurring on a circle about the origin with radius between the sonic and ultimate velocity. This case has been fully explored by Taylor (reference 18). The Ringleb flow (reference 12) and the generalized Ringleb flow as given in this paper are some examples of other types of singularities at the hodograph origin. It is interesting to see that this group can produce transonic flows.

This is the simplest in analysis of the four groups given, because the compressibility effect has no influence on the local character of the singularity at the origin.

(2) One singularity located at the hodograph origin and one or more located on the circle of maximum velocity which is not greater than sonic velocity.

Flows of this type are the impinging jet of subsonic velocity (reference 19 gives the incompressible case) and flow through an aperture (references 2 and 6). Impinging jets can be treated for the compressible flow without difficulty. This group can produce subsonic or at most sonic flows. The compressibility effect will distort the local streamlines of the outer hodograph singularities from the corresponding incompressible ones.

(3) Two singularities, one located at the lowest speed ($q_1 > 0$) and the other located at the highest speed ($q_2 \leqq a$) where the region of hodograph flow is located in the annular region between the singularities.

There are a number of such flows for various contracting channels. One example is discussed in this report. This group can also produce only subsonic or at most sonic flows. It is not too difficult to treat if the incompressible hodograph flow can be expressed analytically. At both singularities the compressibility effect will distort the streamlines locally from the incompressible flow pattern.

(4) One or more hodograph singularities all located inside the flow domain with no streamline tangent to a characteristic.

Hodograph flow corresponding to Borda's mouthpiece (the incompressible case is given in reference 19) may be considered as an example. The hodograph flow corresponding to the physical flow past a circle is another example except this requires a two-sheeted Riemann surface (reference 5).

The flows of this type are much more complicated. The compressibility effect will distort the streamlines in the neighborhood of the singularity if not at the origin. Analytic continuation is always necessary. However, this group could produce transonic flows about a closed body, if no limiting line occurs.

This classification by no means covers all the compressible flows that can be treated by the hodograph methods, being restricted to only those potential flows where Chaplygin's method may be applied. There are many other types of singularities including some located in the supersonic region which extend the flow field into the supersonic range, but such cases are out of the scope of the present treatment.

GENERALIZED RINGLEB FLOW

It is known that a doublet at the origin of the hodograph plane corresponds to an incompressible flow turning about a semi-infinite thin plate in the physical plane. In 1940, Ringleb (reference 12) was the first one to modify such a hodograph doublet with a compressibility effect. He found the streamlines near the tip of the plate could be conformally mapped back to the physical plane only so long as the maximum flow velocity q on the streamline never reaches 1.67 times the stagnation sound velocity $a_o (M = 2.5)$. For higher velocity, the Jacobian $\partial(x,y)/\partial(q,\theta)$ of the transformation relation between the hodograph plane and the physical plane becomes zero along a curved line and the mapping is no longer conformal. At this line the streamlines will form cusps and double back on themselves. No physical flow can be attached to such streamlines. Earlier than 1940, the Clausers (reference 20) found this feature for compressible flow turning within a concave corner. They further discuss the singular behavior of the streamlines and show that the locus of the cusps in the physical plane corresponds to the locus of the points of tangency of the streamlines and the characteristic curves in the hodograph plane. The acceleration is infinite at the cusps. This flow leads to the concepts of the forbidden region of Von Kármán (reference 7) and the limiting lines of Tollmien (reference 16) and Tsien (reference 17). Furthermore, Ringleb was the first to show that smooth transonic flow was possible in a convergent-diverent nozzle formed by the streamlines in the so-called "Ringleb flow."

Figure 3(a) shows that incompressible flow turning a convex corner of angle $2\pi - \alpha$ corresponds to a lemniscate family within the two straight-line asymptotes which contain the angle $\alpha - \pi$ in the hodograph. It is well-known that this incompressible flow can be expressed very simply analytically both in the physical plane and in the hodograph plane. At the sharp convex corner the local flow will reach infinite velocity corresponding to the assumed infinite sound velocity of the incompressible fluid. This flow covers a semi-infinite region in the hodograph bounded by the angle $\alpha - \pi$. However, if the compressibility of the fluid is considered, the sound velocity becomes finite. The possible flow in the hodograph plane is confined within a circle of ultimate velocity q_m and the angle $\alpha - \pi$. Actually, the flow will break down somewhat before the velocity reaches q_m owing to the existence of the limiting line.

As mentioned previously, Kraft and Dibble have studied these flows around convex corners, devoting particular attention to the use of a 60° corner. In the present paper a number of additional examples are given and such features as the location and shape of the limiting lines are studied in greater detail.

Consider the incompressible flow whose complex potential is represented by the analytic function

$$w_i = z^m \tag{11}$$

where $w_i = \phi_i + i\psi_i$ and $z = re^{i\Theta}$ as usually defined. Here Θ is restricted to $0 \leqq \Theta < 2\pi$ which means only the first sheet of the z-plane is considered. The stream function then is

$$\psi_i = r^m \sin m\Theta \tag{12}$$

which gives $\psi_i = 0$ when $\Theta = 0$ and π/m. Thus equation (11) represents the complex potential of a corner flow. Introduce the angle which the flow turns as

$$\alpha = \frac{\pi}{m} \tag{13}$$

Then it is apparent that the corner angle is $2\pi - \alpha$. Consider now only the flow passing a convex corner which corresponds to $\pi < \alpha \leqq 2\pi$ or $1 > m \geqq 1/2$.

The complex velocity is

$$\overline{q}_i = \left|q_i\right|e^{-i\theta} = \frac{dw_i}{dz} = mz^{m-1} = mr^{m-1}e^{i(m-1)\Theta} \tag{14}$$

which shows $\bar{q}_i \longrightarrow \infty$ as $z \longrightarrow 0$ and $\bar{q}_i \longrightarrow 0$ as $z \longrightarrow \infty$ for convex corners. Conversely,

$$z = \left(\frac{\bar{q}_i}{m}\right)^{\frac{1}{m-1}} \tag{15}$$

Thus the flow about the convex corner can be represented in the hodograph plane as

$$w_i = \left(\frac{\bar{q}_i}{m}\right)^{\frac{m}{m-1}} \tag{16}$$

The corresponding stream function in the hodograph plane is

$$\psi_i = -\left(\frac{q_i}{m}\right)^{\frac{m}{m-1}} \sin \frac{m}{m-1} \theta \tag{17}$$

The streamline $\psi_i = 0$ corresponds to the boundary of a concave corner in the hodograph where $\theta = \alpha - \pi \leqq \pi$. The streamlines correspond to leaves of one branch of the lemniscate bounded by that angle, all of which are tangent at the origin. Note that the flow in the physical plane occupies a region of angle α while the flow in the hodograph occupies a region of angle $\alpha - \pi$.

The corner flow has only one singularity, located at the hodograph origin. For the case $\alpha = 3\pi/2$, the hodograph singularity is a quadrupole derived from two sources on a diagonal at 45° and two sinks at -45°. For flow turning around a semi-infinite flat plate $\alpha = 2\pi$, there is a doublet at the origin. These are examples of the first class of hodograph singularities.

Now, following Chaplygin, introduce the compressibility effect into the hodograph equation (equation (4)). Here $n = \pi/(\pi - \alpha)$. The solution ψ_n from equation (7) gives

$$\psi_{\frac{\pi}{\pi-\alpha}}(q) = q^{\frac{\pi}{\pi-\alpha}} F\left(a,b;\ c;\ \frac{q^2}{q_m{}^2}\right) \tag{18}$$

where

$$a + b = \frac{\pi}{\pi - \alpha} - \beta$$

$$ab = -\frac{\beta}{2} \frac{\pi}{\pi - \alpha}\left(\frac{2\pi - \alpha}{\pi - \alpha}\right)$$

$$c = \frac{2\pi - \alpha}{\pi - \alpha}$$

The hypergeometric function $F\left(a,b;\ c;\ \frac{q^2}{{q_m}^2}\right)$ can be represented by the infinite series

$$F\left(a,b;\ c;\ \frac{q^2}{{q_m}^2}\right) = \frac{\Gamma(c)}{\Gamma(a)\Gamma(b)} \sum_{k=0}^{\infty} \frac{\Gamma(a + k)\Gamma(b + k)}{\Gamma(c + k)} \frac{1}{k!}\left(\frac{q}{q_m}\right)^{2k} \tag{19}$$

This series becomes finite if a or b is a negative integer. This fact is utilized for the present numerical calculations.

This solution, equation (18), is convergent for all values of $q < q_m$ and passes continuously into $q^{\frac{\pi}{\pi-\alpha}}$ as $M \longrightarrow 0$ as ensured by equation (10). Introduce $\tau = q^2 / {q_m}^2$. Then this can be written

$$\psi(q) = \left(\frac{1}{q_m}\right)^{\frac{\pi}{\alpha-\pi}} \tau^{\frac{1}{2} \frac{\pi}{\pi-\alpha}} F(a,b;\ c;\ \tau) \tag{20}$$

The solution of $\psi(q,\theta)$ in equation (4) can be written as

$$\psi = A\left(\frac{1}{q_m}\right)^{\frac{\pi}{\alpha-\pi}} \tau^{\frac{1}{2} \frac{\pi}{\pi-\alpha}} F(a,b;\ c;\ \tau) \sin \frac{\pi}{\alpha - \pi}\,\theta \tag{21}$$

Imposing the condition that $\psi \longrightarrow \psi_i$ in equation (17) as $M \longrightarrow 0$, A can be determined as

$$A = \left(\frac{\pi}{\alpha}\right)^{\frac{\pi}{\alpha-\pi}} \tag{22}$$

Thus

$$\psi = \left(\frac{\pi}{\alpha q_m}\right)^{\frac{\pi}{\alpha-\pi}} \tau^{\frac{1}{2}\frac{\pi}{\pi-\alpha}} F(a,b;\ c;\ \tau) \sin \frac{\pi}{\alpha - \pi}\theta \tag{23}$$

which shows the same hodograph singularity at the origin as the incompressible case.

Physical Coordinates

As soon as $\psi_{\frac{\pi}{\pi-\alpha}}$ is known in the hodograph plane, each point in the hodograph can be transformed back to the physical plane by the following relations:

$$\left.\begin{aligned}
x - x_o &= -\frac{q\psi_{\frac{\pi}{\pi-\alpha}}{}' + \frac{\pi}{\alpha - \pi}\psi_{\frac{\pi}{\pi-\alpha}}}{2\tau^{1/2}(1 - \tau)^{\beta}} \frac{\cos\left(1 - \frac{\pi}{\alpha - \pi}\right)\theta}{1 - \frac{\pi}{\alpha - \pi}} + \\
&\quad \frac{q\psi_{\frac{\pi}{\pi-\alpha}}{}' - \frac{\pi}{\alpha - \pi}\psi_{\frac{\pi}{\pi-\alpha}}}{2\tau^{1/2}(1 - \tau)^{\beta}} \frac{\cos\left(1 + \frac{\pi}{\alpha - \pi}\right)\theta}{1 + \frac{\pi}{\alpha - \pi}} \\
y - y_o &= -\frac{q\psi_{\frac{\pi}{\pi-\alpha}}{}' + \frac{\pi}{\alpha - \pi}\psi_{\frac{\pi}{\pi-\alpha}}}{2\tau^{1/2}(1 - \tau)^{\beta}} \frac{\sin\left(1 - \frac{\pi}{\alpha - \pi}\right)\theta}{1 - \frac{\pi}{\alpha - \pi}} + \\
&\quad \frac{q\psi_{\frac{\pi}{\pi-\alpha}}{}' - \frac{\pi}{\alpha - \pi}\psi_{\frac{\pi}{\pi-\alpha}}}{2\tau^{1/2}(1 - \tau)^{\beta}} \frac{\sin\left(1 + \frac{\pi}{\alpha - \pi}\right)\theta}{1 + \frac{\pi}{\alpha - \pi}}
\end{aligned}\right\} \tag{24}$$

where x_o and y_o are integration constants.

The above transformation relations are conformal as long as the streamline is not tangent to a characteristic, where the Jacobian $\partial(x,y)/\partial(q,\theta)$ equals zero. The locus of the points of tangency of the characteristics and the streamlines is called the limiting line by Tollmien (reference 16) and Tsien (reference 17). Its position in the hodograph plane is governed by the following equation:

$$\frac{\partial\psi}{\partial\theta} = \pm 2\tau\sqrt{\frac{1 - \tau}{(2\beta + 1)\tau - 1}}\,\frac{\partial\psi}{\partial\tau} \tag{25}$$

Substituting ψ into equation (17) results in a relation of θ and q which represents the limiting line. Here

$$\cot\left(\frac{\pi}{\pi - \alpha}\,\theta\right) = \pm\frac{2(\pi - \alpha)}{\pi}\sqrt{\frac{1 - \tau}{(2\beta + 1)\tau - 1}}\,\frac{F^*(a,b;\ c;\ \tau)}{F(a,b;\ c;\ \tau)} \tag{26}$$

where

$$F^*(a,b;\ c;\ \tau) = \frac{\Gamma(c)}{\Gamma(a)\Gamma(b)}\sum_{k=0}^{\infty}\frac{\Gamma(a + k)\Gamma(b + k)}{\Gamma(c + k)\Gamma(k + 1)}\left[\frac{\pi}{2(\pi - \alpha)} + k\right]\tau^k \tag{27}$$

With the knowledge of the position of the limiting line in the hodograph and the respective values of $\psi(q,\theta)$ for points upon it, the corresponding limiting line in the physical plane can be found by means of equation (24).

Examples of Generalized Ringleb Flow

It may be of interest to both the theoretical and the practical aerodynamicist to show a few concrete examples of compressible flows derived from the incompressible flow turning around convex corners of different angles. Compressible flows about corners of 46.8°, 90°, 132.9°, and 150.8° are shown. This seemingly arbitrary choice of angles is due to the fact that the corresponding hypergeometric functions have a finite number of terms in the series expansion.

Compressible flow turning about a smooth corner of a 90° angle.- Figure 3(a) shows the incompressible flow about a convex corner of 90° both in the physical plane and in the hodograph plane. (Actually the physical plane has been rotated 45° to emphasize the symmetry of the flow.) The velocity at $\overline{B}$ is infinite so there is an infinite region in the hodograph plane. The hodograph streamlines are one branch of a family of four-leaved lemniscates, all tangent at the origin where the quadrupole singularity is located. It is easy to see that the physical flow at infinity maps to the neighborhood of the hodograph origin $\overline{A},\overline{C}$ where the velocity is zero. Figure 3(b) shows the corresponding compressible flow in both the physical and hodograph planes. This is obtained by Chaplygin's method; for example, take a streamline of incompressible flow, say $\psi = C_1$, and change the velocity magnitude from

$$\left(\frac{\pi}{\alpha q}\right)^{\frac{\pi}{\alpha-\pi}} \text{ to } \left(\frac{\pi}{\alpha q}\right)^{\frac{\pi}{\alpha-\pi}} F\left(a,b;\ c;\ \frac{q^2}{q_m^{\,2}}\right)$$ without changing the phase angle θ

of the velocity. This can be done graphically in the hodograph plane. A few features should be noted. The compressible domain is confined within a circle of radius q_m. The sonic circle divides the hodograph region into two parts, that is, subsonic or elliptic domain $(q < a)$ and supersonic or hyperbolic domain $(q > a)$. Within the subsonic domain the two planes are conformally related. For the supersonic domain, the two planes are still conformally related up to that streamline, say $\psi = C_o^{+}$, which is tangent to a characteristic at A. The corresponding physical streamline (called streamline b later) has a discontinuity in slope at A. To examine this flow in more detail, figure 4(a) shows that compressible flow is physically possible for streamline b and for all streamlines outside it. On streamline b, the slope is discontinuous at A and $C(q/a_o = 1.12)$ which corresponds to the infinite slope of q or infinite acceleration at these points as shown in figure 4(b) and to the points of tangency of the streamline to a characteristic as shown in figure 4(c). It is interesting to find that the maximum obtainable velocity for smooth transonic flow can be found at B where $q/a_o = 1.33$ which is smaller than that of Ringleb flow $(q/a_o = 1.67)$ which is given in reference 7. The limiting lines are shown in both the physical and hodograph planes. The points A and C are the cusps of the limiting lines in the physical planes. The streamlines inside b double back from the limiting line, which is the locus of the streamline cusps. This discussion parallels the work of Ringleb (reference 12) and Von Kármán (reference 7).

However, there are a number of interesting new features to be explored for this case. First, in figure 4(a) the sonic line in the physical plane is always perpendicular to the convex corner symmetrically at D and E. (The dotted corner represents the incompressible boundary; the solid lines, the compressible.) The loop of the sonic line is somewhat of the shape of one branch of a lemniscate, in contrast with the circle in the Ringleb case. The limiting line is also symmetrical and terminates at D and E, normal to the corner. The two inner branches AD and CE of the limiting line lie just inside the sonic line in the physical plane. In the hodograph plane, they are also normal to the boundary and tangent to the sonic circle. However, the b streamline with maximum velocity $q/a_o = 1.33$ begins to be tangent to characteristics at A and C where this streamline has infinite acceleration. Although the limiting line is a smooth symmetrical curve in the hodograph plane, the Jacobian $\partial(x,y)/\partial(q,\theta) = 0$ at A and C and the conformal mapping to the physical plane breaks down. The limiting line in the physical plane has cusps at A and C. Now the hodograph region, a quadrant of the circle of ultimate velocity, is divided into four kinds of regions by the limiting line DACE and the streamline OABCO. (See fig. 4(c).) The region OABC represents a physical field of smooth isentropic flow freely turning the corner. The piece of flow within ODA is also isentropic physical flow, but this flow cannot continue beyond the limiting lines AD or CE unless fluid is properly withdrawn along AD and injected along CE. For example, in figure 4(a) streamline c is first reflected at an oblique angle by the branch of the limiting line AD. The reflected portion corresponds to the portion of the streamline c beyond the limiting line in the hodograph. Then the limiting line reflects c again at another oblique angle. This portion of c lies in the region between the limiting line and the streamline OABCO in the hodograph. Then the streamline c proceeds, doubling back at the limiting line and creating a symmetrical pattern with respect to the center line of the corner. It is interesting to see that the entire hodograph flow in the quadrant of the ultimate-velocity circle maps into a three-sheeted Riemann surface in the physical plane. If a vertical cut of the flow field through D and E is made, one can imagine a threefold sheet as shown in figure 4(d). The branches of the limiting line can be visualized as folding lines of the Riemann surface and each point on c lying between branches of the limiting line has a triple-valued velocity as shown in figure 4(b). This conception may help to explain the mathematical nature of the flow. However, the second and third sheets of the Riemann surface have no physical reality, and only the first sheet corresponds to physically possible flow.

Finally, in the Ringleb flow, the limiting line in the hodograph is monotonic, increasing in curvature up to q_m, and tangent to both the sonic circle (this can be extended in figure 22 of reference 7) and to the ultimate-velocity circle. It resembles a half ellipse. In the case of a 90° corner, the limiting line has two points of inflection although still tangent to both the sonic and the ultimate-velocity circles.

Compressible flow turning about other angles.- The flow turning a 90° angle was described fully in order to show its physical and mathematical features. Three more corner angles, namely 46.8°, 132.9°, and 150.8°, have been calculated and are shown in figures 5 to 7. The notations are consistent with the case of the 90° corner. The acute angle of 46.8° is between the Ringleb case (0° angle) and the 90° angle. Not many new features can be shown in figures 5(a) to 5(e) except that $\left(q/a_o\right)_{max} = 1.50$ at B. A detailed study of these figures can show many features of the Ringleb case which, unfortunately, has not been fully illustrated except in reference 7. Incidentally, the case of Kraft and Dibble (reference 13) has an acute angle of 60° which lies between 0° and 90°. The value of $\left(q/a_o\right)_{max}$ for smooth flow is hard to estimate from their curves. However, it appears to lie between the present values for 46.8° and 90°.

Figures 6(a) to 6(d) show a corner of 132.9°. This case shows additional interesting features. For instance, at F (fig. 6(c)) there is a turning point on the limiting line as it reflects from the straight boundary in the hodograph. For this value of q/a_o, $\psi = 0$ and thus the circular arc GF is also part of the compressible boundary. In the physical plane this section of the boundary is a circular arc where q/a_o is constant (1.00). Although the bounding streamline appears smooth, the enlarged view in figure 6(d) shows that it is not. For the last smooth streamline b, q/a_o is practically constant along that portion of the streamline ABC which is nearly a circular arc. The legs of this streamline are nearly straight lines forming an angle of 139°. The value of q/a_o at B is 0.98.

The limiting line will form a loop at velocities higher than $\left(q/a_o\right)_F$ and is tangent to the ultimate-velocity circle. Thus the limiting line, the streamline b, and the constant-velocity arc GF will divide the sector of the ultimate-velocity circle into six kinds of regions. Then the flow in the physical plane will give a five-sheeted Riemann surface rather than three as before.

The projection of the extended straight-sided boundaries into the field of physical flow and the existence of a rounded constant-velocity tip show this case is essentially different from the preceding angles where the flow is closely related to the Ringleb flow.

Figures 7(a) and 7(b) show the flow about a corner angle of 150.8°. Calculated data are insufficient to predict the shape of the sonic line near D and E. This is the most reasonable guess for the shape. The looped shape of the sonic line is very long and narrow. It is perpendicular to the extended boundaries of the corner angle at D and E. The inner branches of the limiting line coincide with the sonic line near the corner. There are many questions about this flow which have not been settled by the authors. These unsettled data are published purely for stimulation of future investigation.

If this apparent pattern of the sonic loop is extended to the convex corner angle very near but smaller than 180°, it is expe.ted that the loop will become very tall and narrow. In the limit $2\pi - \alpha \longrightarrow 180^{\circ}$, the sonic loop probably collapses into a single straight line perpendicular to the wall, extending to infinity.

When the calculation was undertaken, the authors anticipated finding the relation of the corner angle and maximum q/a_0 in isentropic flow. However, with the few angles studied, $\left(q/a_0\right)_{max}$ does not follow any simple curve, which is all that can be concluded at this time. It seems significant that the maximum velocity point does not shift off the corner center line, and the flow remains symmetrical.

It is apparent that even the simple corner flow deserves more extensive study. It is expected that this simple flow will help in understanding more of compressible flow and its nonlinear equations.

COMPRESSIBLE FLOW THROUGH A TWO-DIMENSIONAL SYMMETRICAL CONTRACTING CHANNEL

The usual requirements for an incompressible flow through a two-dimensional contracting channel are a low, uniform incoming flow velocity and a high, uniform outgoing velocity at the throat. Uniform velocity at the throat cannot be achieved by imposing arbitrary outer boundaries to the channel. However, fortunately, in the hodograph plane, only a source and sink need be specified for such a flow. As far as the corresponding boundary streamlines are concerned, the choice is left entirely to the aerodynamic designer of the channel; he is at liberty to choose those hodograph boundary streamlines which are easy to express analytically. Thus the whole class of incompressible channel flows can be treated favorably by the hodograph method. Along this line of thought, Whitehead, Wu, and Waters (reference 15) show the details of calculating such a symmetrical channel for incompressible flow.[2] However, the method can be applied also to the unsymmetrical channel, if some analytic expression can be found for the channel boundaries.

---

[2]Incidentally, the present authors have found a misstatement in equation (9) in reference 15. The last two terms of equation (9) do not cancel as indicated for the case $k = 2$.

The aim of the present report is to show the extension of this hodograph method to calculate compressible flows through such contracting channels. This is achieved by first expressing the incompressible case in a power series of q and then finding the corresponding compressible flow.

Incompressible Flow through a Channel

The most practical case to consider is the flow through a two-dimensional symmetrical channel. For simplicity in analysis, take the ratio of incoming to outgoing velocity as 1:2 for the incompressible flow. Since the flow is symmetrical with respect to the horizontal axis, only the upper half of the channel is considered. The corresponding boundary streamline in the hodograph is the vertical radius and the 90° arc of a unit circle whose center is the source located at q_1. A sink is located at the end of this arc, namely $q_{2i} = 2q_1$. The other boundary is the image with respect to the horizontal axis. There are two advantages of this choice. First, the whole flow lies in the annular region between the two arcs of radius q_1 and q_2, so that one series can represent the entire flow without the complication of analytic continuation. Second, the incompressible flow can be described in a simple analytic expression in the hodograph plane. Even in this simple case, the computation is quite involved.

There is an inherent disadvantage with this choice; that is, the length of the channel will be infinitely long. The practical application of such a channel seems lost. However, if a reasonable engineering tolerance is admitted to the values of the incoming and outgoing velocities, say 1 percent, the channel length will be finite. With the knowledge of this case, a compressible flow for a finite-length channel can be constructed with the technique of analytic continuation.

Following reference 15, it is not difficult to show that the nondimensional complex potential for the channel incompressible flow with $q_1 = 1$ and $q_{2i} = 2q_1$ can be expressed in the hodograph plane as

$$
\begin{aligned}
w_i &= \frac{4}{\pi} \log_e \frac{\bar{q}_i - 1}{\left(\bar{q}_i - 1\right)^2 - 1} \\
&= \frac{4}{\pi}\left[\log_e \left(\bar{q}_i - 1\right) - \log_e \bar{q}_i - \log_e \left(1 - \frac{\bar{q}_i}{2}\right) - \log_e (-2)\right] \qquad (28)
\end{aligned}
$$

where $\overline{q}_i = q_i e^{-i\theta} = u_i - iv_i$ is the conjugate velocity vector. Since the complex potential is subject to the indeterminancy of a constant, the term $\log_e(-2)$ can be neglected. The second expression is written to show that the hodograph source is $\log_e\left(\overline{q}_i - 1\right)$ and two hodograph sinks are $-\log_e \overline{q}_i$ and $-\log_e\left(1 - \frac{\overline{q}_i}{2}\right)$. All are of the same strength. Of course there is another source of equal strength located at infinity so that the entire flow is steady and in equilibrium. Equation (28) represents the flow field covering the entire hodograph plane. However, if the condition $1 < q < 2$ is imposed, equation (28) can be expanded into a single power series of $\overline{q}_i$. Consequently,

$$w_i = -\frac{4}{\pi}\sum_{n=1}^{\infty}\frac{1}{n}\left(\overline{q}_i^{\,-n} - 2^{-n}\overline{q}_i^{\,n}\right) \tag{29}$$

If $\overline{q}_i$ is expressed explicitly in terms of q_i and θ,

$$w_i = -\frac{4}{\pi}\sum_{n=1}^{\infty}\frac{1}{n}\left(q_i^{-n}e^{in\theta} - 2^{-n}q_i^{n}e^{-in\theta}\right) \tag{30}$$

Compressible Flow through a Channel

Now the compressibility effect can be considered. Chaplygin's procedure shows that, for each value of n, the incompressible velocity $q_i^{\pm n}$ in the stream function will change to a new velocity magnitude $\psi_{\pm n}(\tau)/\psi_{\pm n}(\tau_1)$ while the angularity θ remains the same.[3] Being linear in the hodograph plane, all the solutions are superposable. Thus the nondimensional stream function is

$$\psi_c = -\frac{4}{\pi}\sum_{n=1}^{\infty}\frac{1}{n}\left[\frac{\psi_{-n}(\tau)}{\psi_{-n}(\tau_1)} + 2^{-n}\frac{\psi_n(\tau)}{\psi_n(\tau_1)}\right]\sin n\theta \tag{31}$$

[3] If $q_{i2} = 1$ is chosen, $\psi_{\pm n}(\tau)/\psi_{\pm n}(\tau_2)$ should be used to replace $\psi_{\pm n}(\tau)/\psi_{\pm n}(\tau_1)$ and τ_1 should be replaced everywhere in the later expressions.

Of course, the above ψ_c can be considered as the imaginary part of the complex function

$$w_c = -\frac{4}{\pi}\sum_{n=1}^{\infty}\frac{1}{n}\left[\frac{\psi_{-n}(\tau)}{\psi_{-n}(\tau_1)}\, e^{in\theta} - 2^{-n}\frac{\psi_n(\tau)}{\psi_n(\tau_1)}\right]\sin n\theta \qquad (32)$$

but the real part of w_c is no longer a solution of the potential ϕ_c as in the case of incompressible flow. It is well-known that ϕ_c and ψ_c are not conjugate functions in compressible flow. It should be remarked than an infinite number of channel shapes of compressible flow can be constructed from the same incompressible flow by choosing some function $f_{2n}(\tau_1)$ to replace $\psi_{\pm n}(\tau_1)$ so that $f_{\pm n}(\tau_1) \longrightarrow q_1^{\pm n}$ as $M \longrightarrow 0$.

Physical Coordinates

As shown in references 4 and 14, introduce the physical coordinate $Z = X_n + iY_n$ to correspond to each eigenvalue n. Then

$$Z = \sum_{n=1}^{\infty}\left(Z_n - Z_{on}\right) \qquad (Z_{on}\text{'s are constants}) \qquad (33)$$

It can be shown that for $n \neq 1$

$$\begin{aligned}
Z_n &= X_n + iY_n \\
&= \frac{4}{\pi}\frac{1}{n\tau^{1/2}(1-\tau)^{\beta}}\left\{\frac{e^{(1-n)i\theta}}{(1-n)\psi_{-n}(\tau_1)}\left[-\frac{n}{2}\psi_{-n}(\tau) - \tau\psi_{-n}'(\tau)\right] + \right. \\
&\quad \frac{2^{-n}e^{(1+n)i\theta}}{(1+n)\psi_n(\tau_1)}\left[\frac{n}{2}\psi_n(\tau) - \tau\psi_n'(\tau)\right] + \\
&\quad \frac{e^{(1+n)i\theta}}{(1+n)\psi_{-n}(\tau_1)}\left[-\frac{n}{2}\psi_{-n}(\tau) + \tau\psi_{-n}'(\tau)\right] - \\
&\quad \left.\frac{2^{-n}e^{-(1-n)i\theta}}{(1-n)\psi_n(\tau_1)}\left[\frac{n}{2}\psi_n(\tau) + \tau\psi_n'(\tau)\right]\right\}
\end{aligned} \qquad (34)$$

where

$$\psi_{\pm n}'(\tau) = \frac{d}{d\tau}\left[\psi_{\pm n}(\tau)\right]$$

For $n = 1$

$$Z_1 = X_1 + iY_1$$

$$= \frac{1}{\pi}\left\{\frac{1}{\psi_1(\tau_1)}\left[1 - \frac{1 - (1 - \tau)^{\beta+1}}{(\beta + 1)\tau(1 - \tau)^{\beta}}\right] - \right.$$

$$\left.\frac{1}{\tau\psi_{-1}(\tau_1)}\left[\frac{3\beta + 2}{\beta + 1}\frac{1}{(1 - \tau)^{\beta}} - \frac{\beta}{\beta + 1}(1 + \beta\tau)\right]\right\} e^{i2\theta} +$$

$$\frac{1}{\pi}\left[\frac{1}{\psi_1(\tau_1)} + \frac{\beta}{\psi_{-1}(\tau_1)}\right]\log_e (\tau e^{-2i\theta}) +$$

$$\frac{1}{\pi}\left[\frac{1}{\psi_1(\tau_1)} - \frac{1}{\psi_{-1}(\tau)}(3\beta + 2)\right]\frac{(2\beta + 1)}{(\beta + 1)}\left[\frac{1}{(1 - \tau)^{\beta}} - 1\right] -$$

$$\frac{1}{\pi}\left[\frac{2\beta}{\psi_1(\tau_1)(\beta + 1)} - \frac{2\beta(3\beta + 2)}{\psi_{-1}(\tau_1)(\beta + 1)}\right]g(\tau) - \frac{2\beta}{\pi\psi_{-1}(\tau_1)}\log_e \tau \tag{35}$$

where

$$\psi_1(\tau) = \frac{\tau^{-1/2}}{\beta + 1}\left[1 - (1 - \tau)^{\beta+1}\right]$$

$$\psi_{-1}(\tau) = \tau^{-1/2} + \frac{\beta}{2}\,\psi_1(\tau)$$

$$g(\tau) = \frac{1}{2}\int_0^{\tau}\left[\frac{1 - (2\beta + 1)\tau}{(1 - \tau)^{\beta+1}} - 1\right]\frac{d\tau}{\tau}$$

Values of the function $g(\tau)$ are shown in table 5 of reference 14.

Numerical Calculation of Compressible Channel Flow

A numerical calculation for the above analysis was made for the case $\tau_1 = 0.02$ $\left(M_1 = 0.320,\ q_1 = 354.0 \text{ ft/sec, and } a_o = 1117.4 \text{ ft/sec}\right)$. For comparison, the incompressible channel flow with the same inlet velocity was also made. The hodograph boundary and the channel geometry for both flows are shown in figures 8(a) and 8(b). For both cases, the hodograph source is located at A $\left(q_1 = 354.0 \text{ ft/sec}\right)$. The incompressible hodograph sink is $B_i\left(q_{2i} = 2q_1\right)$. The streamline boundary $\psi = 2$ is chosen for both the compressible and incompressible cases. Note that, for the same q_1, q_{2c} is much larger than $2q_1$. (In fact, $M_2 = 0.787$ and $q_{2c} = 825$ ft/sec.) A few points in figures 8(a) and 8(b) need some clarification. Far upstream, both channels have the same width 4, and $\psi_i = \psi_c = 2$ on the upper boundaries because both channels have identical inlet conditions. The points of inflection of the incompressible and compressible channel boundary are I_i and I_c, respectively. As expected from the compressibility effect, the compressible flow channel is wider than the incompressible one. However, if outlet conditions of both channels were matched $\left(q_{2c} = q_{2i}\right)$, the incompressible channel would be wider than the compressible one.

The convergence of the series solution in ψ_c is extremely slow. It is difficult to obtain a reasonably good summation with n up to 15 as given in reference 9, particularly when the velocity phase angle is very small and the Mach number is nearly sonic. Shanks' method (reference 10) makes possible a closer approximation to the value of ψ_c with so few terms. It had been planned to calculate the compressible channel flow with sonic throat velocity. However, owing to the insufficient data in the table and slow convergence of the series, this project was not carried through although the authors fully realize the engineering importance of a contracting channel with sonic throat. The example given shows it is possible to obtain an exact solution for compressible channel flow and that this method can be applied to the sonic case when sufficient data are available.

Figure 9 shows the various streamlines in the $\tau\theta$-plane. The maximum τ at the throat is 0.11 ($M = 0.787$). Owing to the slow convergence of the infinite series of ψ_c, τ_{max} at the channel throat is only reasonably correct and may be subject to a small error. It is noticed that the maximum velocity angle θ of each streamline occurs nearly at the same value, $\tau = 0.042$, where the points of inflection are located.

Figures 10(a) and 10(b) show the position of the boundary streamlines of both the compressible and incompressible cases expressed in terms of $x = x(\tau)$ and $y = y(\tau)$. In the compressible case, $\tau = q_c^2/q_m^2$ is already defined. For the incompressible case, τ is directly proportional to the square of the incompressible flow velocity where the constant of proportionality is taken as $\frac{1}{(\gamma - 1)a_o^2} = \frac{1}{q_m^2}$ so that $\tau = q_i^2/q_m^2$. Then τ is a good measure of relative velocity magnitudes in the compressible and incompressible flows. It is difficult to calculate both $x(\tau)$ and $y(\tau)$ in the compressible flow. The dashed line of ψ_c means the best approximation so far. Similarly the x-coordinates of the center streamlines $\psi_i = 0$ and $\psi_c = 0$ as a function of τ are also plotted in figure 11. With the data along the streamlines $\psi_c = 0$, 1, and 2 the approximate contour lines of constant velocity for the compressible flow channel near the point of inflection I_c can be shown (fig. 12). To compare details of the channel wall, the boundary line of the incompressible flow is translated so that its point of inflection I_i coincides with I_c (fig. 13). It shows that the channel area of the compressible case decreases slower with x than the incompressible one in the neighborhood of the point of inflection.

The Johns Hopkins University
Baltimore, Md., May 28, 1952

APPENDIX A

EXTENSION OF HUCKEL'S TABLES FOR SUBSONIC RANGE

For the contracting channel, the whole flow region covers only a small range of τ. Many values of the Chaplygin function for τ intermediate to the arguments given in Huckel's tables (reference 9) are needed to determine the flow field accurately. In order to avoid interpolating every time, each subsonic section of the tables was interpolated as a unit so the Chaplygin functions can be read directly as needed. These values are given in tables 1 to 4. The accuracy of the values should be at worst only one place less than the figures in the original tables.

As has been noted in the errata, the headings $dY_k/d\tau$ and $dY_{-k}/d\tau$ for tables 3 and 4 of Huckel's report are in error. To obtain the actual derivative, each tabulated value should be multiplied by $-k\beta/2$. The values here listed in table 3 and table 4 are the derivatives and are denoted $Y_k'(\tau)$ and $Y_{-k}'(\tau)$ to prevent confusion with the headings in the original tables. Otherwise the arrangement and notation correspond exactly to Huckel's tables.

APPENDIX B

SYMBOLS

a	sound velocity $\left(\sqrt{\frac{\gamma p}{\rho}} = \sqrt{\gamma RT}\right)$
a_o	stagnation sound velocity $\left(\sqrt{\frac{\gamma p_o}{\rho_o}} = \sqrt{\gamma RT_o}\right)$
a	typical smooth streamline
b	streamline of smooth isentropic flow with maximum velocity
c	typical streamline that doubles back at limiting lines
k	index number for summation
m	index power
n	eigenvalue
p	local pressure
p_o	stagnation pressure
q	velocity magnitude
q_i	velocity magnitude of incompressible flow
q_c	velocity magnitude of compressible flow
$\overline{q}_i$	incompressible conjugate velocity vector $\left(\frac{dw_i}{dz} = u_i - iv_i\right)$
q_m	ultimate velocity $\left(a_o\sqrt{\frac{2}{\gamma - 1}}\right)$
q_1	inlet velocity

q_2	throat velocity
q_{2i}	incompressible throat velocity
q_{2c}	compressible throat velocity
u,v	velocity components
u_i,v_i	incompressible velocity components
w_i	complex potential
w_c	complex variable function, the imaginary part of which is the stream function
x,y	rectangular coordinates
z	complex variable $\left(re^{i\theta}\right)$
A,C	locations of cusps of limiting line
B	location of maximum velocity in smooth isentropic flow
D,E	termination of sonic line and limiting line at convex corner
F,G	intersections of limiting line with convex corner
$F\left(a,b;\ c;\ \frac{q^2}{{q_m}^2}\right)$	hypergeometric function
I_i	point of inflection of channel boundary for incompressible flow
I_c	point of inflection of channel boundary for compressible flow
M	Mach number
R	molar gas constant

T	temperature
T_o	stagnation temperature
X_n, Y_n	physical coordinate corresponding to each eigenvalue n
$Z_n = X_n + iY_n$	
Z	physical coordinates corresponding to a hodograph point
α	angle covered by flow
$2\pi - \alpha$	angle of convex corner
$\beta = \dfrac{1}{\gamma - 1}$	
γ	specific heat ratio; for air $\gamma = 1.4$
θ	velocity phase angle
θ_i	phase angle of incompressible velocity
θ_c	phase angle of compressible velocity
ρ	local density
ρ_o	stagnation density
$\tau = \dfrac{q^2}{{q_m}^2} = \dfrac{2}{\gamma - 1} \dfrac{q^2}{{a_o}^2}$	
ϕ_i	potential in incompressible flow
ϕ_c	potential in compressible flow
ψ	stream function
ψ_i	incompressible stream function

ψ_c compressible stream function

$\psi_{\pm n}(q) = q^{\pm n}F\left(a_n, b_n; c_n; \tau\right)$

Θ phase angle of complex variable

REFERENCES

1. Molenbroek, P.: Über einige Bewegungen eines Gases mit Annahme eines Geschwindigkeitspotentials. Archiv Math. und Phys., Bd. 2, Heft 9, 1890, p. 157.

2. Chaplygin, S. A.: On Gas Jets. Sci. Ann. Imperial Univ. Moscow, Physico-Mathematical Div., No. 21, Moscow, 1904. (Available in translation as NACA TM 1063.)

3. Tsien, Hsue-Shen, and Kuo, Yung-Huai: Two-Dimensional Irrotational Mixed Subsonic and Supersonic Flow of a Compressible Fluid and the Upper Critical Mach Number. NACA TN 995, 1946.

4. Lighthill, M. J.: The Hodograph Transformation in Tran-Sonic Flow. Parts I-III. Proc. Roy. Soc. (London), ser. A, vol. 191, no. 1026, 1947, pp. 323-369.

5. Cherry, T. M.: Flow of a Compressible Fluid about a Cylinder. Part I. Proc. Roy. Soc. (London), ser. A, vol. 192, no. 1028, Dec. 23, 1947, pp. 45-79; Part II. Flow with Circulation. Proc. Roy. Soc. (London), ser. A, vol. 196, no. 1044, Feb. 22, 1949, pp. 1-31.

6. Chang, Chieh-Chien: General Consideration of Problems in Compressible Flow Using the Hodograph Method. NACA TN 2582, 1952.

7. Von Kármán, Th.: Compressibility Effects in Aerodynamics. Jour. Aero. Sci., vol. 8, no. 9, July 1941, pp. 337-356.

8. Guderley, K. Gottfried, and Yoshihara, Hideo: The Flow over a Wedge Profile at Mach Number One. Tech. Rep. No. 5783, Air Materiel Command, Army Air Forces, July 1949.

9. Huckel, Vera: Tables of Hypergeometric Functions for Use in Compressible-Flow Theory. NACA TN 1716, 1948.

10. Shanks, Daniel: An Analogy between Transients and Mathematical Sequences and Some Nonlinear Sequence-to-Sequence Transforms Suggested by It. Part I. Memo. 9994, Naval Ord. Lab., July 26, 1949.

11. Cherry, T. M.: Uniform Asymptotic Formulae for Functions with Transition Points. Trans. Am. Math. Soc., vol. 68, no. 2, March 1950, pp. 224-257.

12. Ringleb, Friedrich: Exakte Lösungen der Differential-gleichungen einer adiabatischen Gasströmung. Z.a.M.M., Bd. 20, Heft 4, Aug. 1940, pp. 185-198. (Available as R.T.P. Translation No. 1609, British Ministry of Aircraft Production.)

13. Kraft, Hans, and Dibble, Charles G.: Some Two-Dimensional Adiabatic Compressible Flow Patterns. Jour. Aero. Sci., vol. 11, no. 4, Oct. 1944, pp. 283-298.

14. Garrick, I. E., and Kaplan, Carl: On the Flow of a Compressible Fluid by the Hodograph Method. II - Fundamental Set of Particular Flow Solutions of the Chaplygin Differential Equation. NACA Rep. 790, 1944.

15. Whitehead, L. G., Wu, L. Y., and Waters, M. H. L.: Contracting Ducts of Finite Length. Aero. Quart., vol. 2, pt. 4, Feb. 1951, pp. 254-271.

16. Tollmien, W.: Limit Lines in Adiabatic Potential Flows. R.T.P. Translation No. 1610, British Ministry of Aircraft Production. (From Z.a.M.M., Bd. 21, Heft 3, June 1941, pp. 140-152.)

17. Tsien, Hsue-shen: The "Limiting Line" in Mixed Subsonic and Supersonic Flow of Compressible Fluids. NACA TN 961, 1944.

18. Taylor, G. I.: Recent Work on the Flow of Compressible Fluids. Jour. London Math. Soc., vol. 5, 1930, pp. 224-240.

19. Milne-Thomson, L. M.: Theoretical Hydrodynamics. Second ed., The Macmillan Co., 1950.

20. Clauser, M. U., and Clauser, F. H.: New Method of Solving the Equations for the Flow of Compressible Fluids. Doctorate Thesis, C.I.T., 1937.

TABLE 1.- $Y_k(\tau)$ FOR VARIOUS VALUES OF k

τ	Y_1	Y_2	Y_3	Y_4	Y_5	Y_6	Y_7	Y_8
0.02	0.97525	0.95087	0.92700	0.90369	0.88093	0.85873	0.83708	0.81596
.022	.97280	.94606	.91991	.89446	.86966	.84553	.82207	.79923
.024	.97036	.94126	.91287	.88530	.85850	.83250	.80728	.78278
.026	.96792	.93648	.90587	.87621	.84745	.81963	.79270	.76661
.028	.96549	.93171	.89891	.86718	.83651	.80691	.77833	.75072
.03	.96306	.92695	.89198	.85822	.82568	.79434	.76416	.73511
.032	.96064	.92221	.88509	.84934	.81496	.78193	.75021	.71977
.034	.95822	.91749	.87824	.84053	.80435	.76969	.73647	.70470
.036	.95581	.91279	.87143	.83179	.79385	.75760	.72294	.68989
.038	.95340	.90811	.86466	.82311	.78345	.74566	.70962	.67534
.04	.95099	.90346	.85792	.81449	.77316	.73386	.69651	.66104
.042	.94859	.89882	.85122	.80594	.76298	.72221	.68359	.64699
.044	.94619	.89419	.84456	.79746	.75290	.71071	.67086	.63319
.046	.94380	.88958	.83794	.78905	.74292	.69936	.65832	.61964
.048	.94142	.88498	.83136	.78072	.73304	.68816	.64598	.60634
.05	.93905	.88039	.82481	.77245	.72326	.67710	.63383	.59328
.052	.93668	.87582	.81830	.76424	.71358	.66618	.62187	.58045
.054	.93431	.87127	.81183	.75609	.70400	.65540	.61009	.56785
.056	.93195	.86674	.80539	.74801	.69452	.64476	.59849	.55547
.058	.92959	.86223	.79899	.74000	.68515	.63426	.58706	.54331
.06	.92723	.85773	.79262	.73205	.67588	.62389	.57581	.53138
.062	.92488	.85325	.78629	.72416	.66671	.61366	.56474	.51967
.064	.92254	.84878	.78000	.71634	.65763	.60356	.55384	.50817
.066	.92020	.84433	.77375	.70858	.64864	.59359	.54311	.49688
.068	.91787	.83990	.76753	.70088	.63974	.58375	.53256	.48580
.07	.91554	.83549	.76135	.69325	.63094	.57405	.52218	.47492
.072	.91322	.83109	.75520	.68568	.62223	.56448	.51196	.46424
.074	.91090	.82671	.74909	.67817	.61362	.55503	.50190	.45376
.076	.90858	.82234	.74302	.67072	.60510	.54570	.49200	.44348
.078	.90627	.81799	.73698	.66333	.59667	.53650	.48226	.43340
.08	.90396	.81366	.73098	.65600	.58834	.52742	.47268	.42352
.082	.90166	.80934	.72501	.64873	.58010	.51847	.46325	.41383
.084	.89936	.80504	.71901	.64152	.57195	.50964	.45397	.40432
.086	.89707	.80076	.71317	.63437	.56388	.50093	.44484	.39498
.088	.89479	.79649	.70731	.62729	.55589	.49233	.43586	.38580
.09	.89251	.79224	.70149	.62027	.54798	.48384	.42704	.37679
.092	.89023	.78800	.69570	.61331	.54016	.47547	.41836	.36796
.094	.88796	.78378	.68994	.60640	.53243	.46722	.40982	.35931
.096	.88569	.77958	.68421	.59954	.52479	.45909	.40142	.35083
.098	.88343	.77539	.67852	.59274	.51724	.45107	.39316	.34253
.10	.88117	.77122	.67286	.58600	.50979	.44315	.38503	.33439
.102	.87892	.76706	.66724	.57932	.50241	.43534	.37704	.32641
.104	.87667	.76292	.66165	.57270	.49510	.42765	.36919	.31858
.106	.87443	.75880	.65609	.56613	.48787	.42007	.36147	.31090
.108	.87219	.75469	.65057	.55962	.48073	.41259	.35388	.30337
.11	.86996	.75060	.64508	.55316	.47367	.40521	.34641	.29599
.112	.86773	.74652	.63963	.54676	.46669	.39794	.33907	.28875
.114	.86551	.74246	.63421	.54041	.45979	.39077	.33186	.28167
.116	.86329	.73841	.62882	.53412	.45297	.38371	.32477	.27473
.118	.86107	.73438	.62346	.52789	.44622	.37674	.31781	.26793
.12	.85886	.73037	.61813	.52171	.43955	.36987	.31097	.26127
.122	.85665	.72637	.61283	.51558	.43296	.36310	.30425	.25475
.124	.85445	.72238	.60757	.50951	.42645	.35643	.29764	.24836
.126	.85226	.71841	.60235	.50349	.42001	.34985	.29114	.24210
.128	.85007	.71446	.59716	.49752	.41364	.34337	.28476	.23596
.13	.84789	.71053	.59201	.49160	.40733	.33699	.27849	.22995
.132	.84571	.70661	.58689	.48573	.40110	.33070	.27233	.22407
.134	.84353	.70270	.58180	.47991	.39495	.32450	.26628	.21831
.136	.84136	.69881	.57674	.47415	.38887	.31839	.26034	.21267
.138	.83919	.69493	.57170	.46845	.38287	.31237	.25451	.20715
.14	.83703	.69107	.56668	.46280	.37695	.30645	.24879	.20176
.142	.83487	.68722	.56170	.45720	.37110	.30062	.24317	.19648
.144	.83272	.68339	.55676	.45164	.36531	.29487	.23765	.19131
.146	.83057	.67958	.55186	.44613	.35958	.28920	.23222	.18625
.148	.82843	.67578	.54699	.44067	.35391	.28362	.22689	.18129
.15	.82629	.67200	.54215	.43526	.34832	.27811	.22166	.17644
.152	.82416	.66823	.53734	.42990	.34280	.27269	.21652	.17170
.154	.82203	.66447	.53256	.42459	.33735	.26736	.21148	.16706
.156	.81991	.66073	.52781	.41933	.33196	.26211	.20654	.16252
.158	.81779	.65701	.52308	.41412	.32664	.25694	.20169	.15808
.16	.81567	.65331	.51838	.40896	.32138	.25185	.19694	.15375
.162	.81356	.64962	.51372	.40384	.31619	.24684	.19228	.14951
.164	.81145	.64594	.50909	.39877	.31106	.24191	.18770	.14536
.166	.80935	.64227	.50449	.39375	.30599	.23705	.18320	.14130

NACA

TABLE 1.- $Y_k(\tau)$ FOR VARIOUS VALUES OF k - Concluded

τ	Y_9	Y_{10}	Y_{11}	Y_{12}	Y_{13}	Y_{14}	Y_{15}
0.02	0.79537	0.77530	0.75573	0.73666	0.71806	0.69993	0.68226
.022	.77704	.75549	.73447	.71405	.69428	.67498	.65627
.024	.75906	.73609	.71372	.69203	.67114	.65076	.53108
.026	.74142	.71709	.69346	.67060	.64863	.62727	.60669
.028	.72412	.69849	.67368	.64975	.62675	.60450	.58309
.03	.70716	.68028	.65438	.62947	.60551	.58246	.56029
.032	.69054	.66249	.63556	.60976	.58491	.56113	.53829
.034	.67425	.64511	.61722	.59060	.56495	.54051	.51709
.036	.65829	.62814	.59935	.57196	.54562	.52060	.49668
.038	.64266	.61156	.58195	.55383	.52692	.50139	.47706
.04	.62736	.59538	.56502	.53619	.50884	.48287	.45823
.042	.61237	.57957	.54853	.51904	.49129	.46493	.44001
.044	.59768	.56411	.53245	.50238	.47424	.44755	.42239
.046	.58328	.54898	.51675	.48620	.45768	.43072	.40537
.048	.56915	.53418	.50141	.47049	.44161	.41444	.38895
.05	.55530	.51972	.48642	.45523	.42604	.39871	.37313
.052	.54174	.50560	.47183	.44040	.41097	.38352	.35787
.054	.52847	.49182	.45764	.42599	.39638	.36885	.34317
.056	.51548	.47837	.44385	.41198	.38226	.35469	.32903
.058	.50277	.46524	.43045	.39837	.36859	.34102	.31545
.06	.49034	.45244	.41745	.38515	.35534	.32782	.30244
.062	.47816	.43995	.40478	.37231	.34249	.31507	.28987
.064	.46623	.42774	.39242	.35984	.33003	.30276	.27774
.066	.45454	.41580	.38035	.34774	.31796	.29088	.26604
.068	.44309	.40413	.36857	.33601	.30638	.27941	.25477
.07	.43189	.39272	.35702	.32466	.29516	.26834	.24994
.072	.42093	.38159	.34591	.31364	.28428	.25765	.23351
.074	.41020	.37074	.33506	.30293	.27374	.24734	.22348
.076	.39970	.36017	.32453	.29252	.26353	.23740	.21384
.078	.38944	.34988	.31431	.28241	.25366	.22782	.20459
.08	.37941	.33985	.30439	.27260	.24412	.21860	.19574
.082	.36960	.33006	.29472	.26309	.23489	.20971	.18721
.084	.35999	.32050	.28530	.25387	.22596	.20113	.17899
.086	.35058	.31116	.27613	.24494	.21733	.19285	.17108
.088	.34138	.30205	.26721	.23630	.20900	.18487	.16348
.09	.33238	.29315	.25852	.22795	.20098	.17719	.15620
.092	.32358	.28448	.25008	.21985	.19323	.16979	.14920
.094	.31498	.27603	.24188	.21199	.18573	.16267	.14247
.096	.30657	.26780	.23392	.20436	.17848	.15582	.13601
.098	.29835	.25979	.22620	.19696	.17145	.14921	.12983
.10	.29032	.25201	.21871	.18978	.16465	.14284	.12391
.102	.28247	.24442	.21143	.18283	.15809	.13671	.11822
.104	.27480	.23701	.20435	.17610	.15177	.13081	.11275
.106	.26730	.22978	.19746	.16959	.14568	.12514	.10750
.108	.25997	.22273	.19076	.16331	.13982	.11970	.10248
.11	.25280	.21585	.18426	.15725	.13419	.11449	.09767
.112	.24580	.20915	.17795	.15138	.12874	.10948	.09307
.114	.23896	.20263	.17183	.14568	.12347	.10465	.08865
.116	.23228	.19629	.16589	.14016	.11838	.10000	.08441
.118	.22576	.19014	.16013	.13482	.11347	.09552	.08035
.12	.21940	.18417	.15455	.12965	.10874	.09119	.07646
.122	.21319	.17835	.14913	.12465	.10418	.08704	.07273
.124	.20712	.17267	.14387	.11982	.09979	.08307	.06916
.126	.20119	.16713	.13876	.11516	.09556	.07927	.06575
.128	.19540	.16174	.13381	.11066	.09149	.07563	.06250
.13	.18975	.15649	.12901	.10631	.08759	.07214	.05941
.132	.18424	.15139	.12436	.10211	.08383	.06879	.05645
.134	.17886	.14643	.11985	.09805	.08020	.06557	.05361
.136	.17361	.14161	.11548	.09413	.07670	.06247	.05088
.138	.16849	.13693	.11124	.09034	.07333	.05950	.04827
.14	.16349	.13238	.10714	.08667	.07008	.05665	.04578
.142	.15861	.12796	.10317	.08313	.06696	.05392	.04340
.144	.15385	.12366	.09932	.07972	.06996	.05131	.04113
.146	.14921	.11948	.09559	.07643	.06108	.04881	.03897
.148	.14469	.11541	.09198	.07326	.05832	.04642	.03692
.15	.14029	.11146	.08849	.07021	.05567	.04413	.03497
.152	.13600	.10762	.08511	.06726	.05312	.04194	.03311
.154	.13182	.10389	.08184	.06441	.05067	.03984	.03133
.156	.12774	.10027	.07867	.06166	.04831	.03783	.02963
.158	.12376	.09676	.07560	.05901	.04605	.03591	.02801
.16	.11987	.09335	.07264	.05647	.04388	.03407	.02645
.162	.11609	.09004	.06978	.05402	.04180	.03231	.02497
.164	.11241	.08683	.06701	.05166	.03980	.03063	.02357
.166	.10882	.08371	.06433	.04938	.03788	.02903	.02224

NACA

TABLE 2.- $Y_{-k}(\tau)$ FOR VARIOUS VALUES OF k

τ	Y_{-1}	Y_{-2}	Y_{-3}	Y_{-4}	Y_{-5}	Y_{-6}	Y_{-7}	Y_{-8}
0.02	1.02438	1.06098	1.08708	1.11260	1.14016	1.16911	1.19910	1.22999
.022	1.02674	1.06790	1.09735	1.12550	1.15603	1.18835	1.22185	1.25673
.024	1.02909	1.07489	1.10793	1.13885	1.17243	1.20817	1.24537	1.28428
.026	1.03144	1.08196	1.11882	1.15265	1.18936	1.22859	1.26967	1.31269
.028	1.03378	1.08911	1.13002	1.16690	1.20683	1.24966	1.29476	1.34201
.03	1.03611	1.09633	1.14154	1.18160	1.22485	1.27139	1.32064	1.37229
.032	1.03843	1.10362	1.15338	1.19677	1.24342	1.29377	1.34730	1.40354
.034	1.04074	1.11098	1.16554	1.21241	1.26255	1.31680	1.37475	1.43577
.036	1.04303	1.11841	1.17803	1.22852	1.28224	1.34049	1.40299	1.46899
.038	1.04530	1.12591	1.19085	1.24510	1.30249	1.36486	1.43202	1.50326
.04	1.04755	1.13347	1.20400	1.26215	1.32332	1.38993	1.46184	1.53869
.042	1.04979	1.14107	1.21746	1.27979	1.34490	1.41950	1.49276	1.57532
.044	1.05202	1.14870	1.23123	1.29804	1.36728	1.44284	1.52482	1.61420
.046	1.05425	1.15635	1.24531	1.31689	1.39049	1.47079	1.55812	1.65333
.048	1.05647	1.16402	1.25971	1.33634	1.41456	1.49978	1.59270	1.69396
.05	1.05869	1.17171	1.27443	1.35639	1.43954	1.52984	1.62862	1.73604
.052	1.06089	1.17943	1.28945	1.37706	1.46541	1.56100	1.66594	1.77982
.054	1.06307	1.18717	1.30477	1.39835	1.49218	1.59331	1.70467	1.82540
.056	1.06524	1.19493	1.32138	1.42028	1.51985	1.62685	1.74482	1.87283
.058	1.06740	1.20270	1.33628	1.44286	1.54842	1.66166	1.78640	1.92251
.06	1.06954	1.21049	1.35248	1.46612	1.57789	1.69775	1.82943	1.97447
.062	1.07167	1.21829	1.36896	1.49006	1.60849	1.73524	1.87427	2.02871
.064	1.07379	1.22608	1.38571	1.51468	1.64027	1.77432	1.92121	2.08523
.066	1.07590	1.23385	1.40274	1.53999	1.67325	1.81503	1.97037	2.14405
.068	1.07801	1.24161	1.42004	1.56598	1.70745	1.85749	2.02184	2.20517
.07	1.08011	1.24935	1.43760	1.59265	1.74290	1.90171	2.07570	2.26864
.072	1.08219	1.25708	1.45541	1.62003	1.77959	1.94773	2.13196	2.33526
.074	1.08426	1.26480	1.47346	1.64813	1.81753	1.99557	2.19068	2.40543
.076	1.08632	1.27252	1.49175	1.67695	1.85672	2.04534	2.25190	2.47930
.078	1.08837	1.28023	1.51028	1.70649	1.89716	2.09707	2.31566	2.55703
.08	1.09040	1.28793	1.52903	1.73675	1.93888	2.15078	2.38198	2.63886
.082	1.09242	1.29560	1.54799	1.76772	1.98203	2.20669	2.45151	2.72484
.084	1.09443	1.30323	1.56716	1.79940	2.02664	2.26495	2.52450	2.81506
.086	1.09643	1.31082	1.58653	1.83178	2.07273	2.32566	2.60109	2.90958
.088	1.09842	1.31837	1.60610	1.86486	2.12031	2.38886	2.68141	3.00850
.09	1.10041	1.32588	1.62588	1.89864	2.16941	2.45456	2.76563	3.11187
.092	1.10238	1.33336	1.64582	1.93311	2.22002	2.52284	2.85376	3.22104
.094	1.10434	1.34081	1.66592	1.96827	2.27213	2.59374	2.94577	3.33631
.096	1.10629	1.34822	1.68618	2.00413	2.32574	2.66729	3.04182	3.45783
.098	1.10823	1.35559	1.70660	2.04068	2.38085	2.74351	3.14190	3.58590
.10	1.11015	1.36292	1.72716	2.07790	2.43746	2.82240	3.24609	3.72071
.102	1.11206	1.37020	1.74785	2.11576	2.49566	2.90426	3.35518	3.86242
.104	1.11396	1.37743	1.76866	2.15426	2.55547	2.98917	3.46938	4.01129
.106	1.11585	1.38461	1.78959	2.19340	2.61690	3.07718	3.58879	4.16756
.108	1.11774	1.39174	1.81064	2.23318	2.67997	3.16835	3.71350	4.33157
.11	1.11962	1.39882	1.83181	2.27359	2.74469	3.26269	3.84363	4.50372
.112	1.12149	1.40585	1.85306	2.31457	2.81096	3.36020	3.97926	4.68443
.114	1.12334	1.41282	1.87438	2.35612	2.87877	3.46088	4.11945	4.87414
.116	1.12518	1.41973	1.89577	2.39823	2.94812	3.56473	4.26631	5.07333
.118	1.12701	1.42658	1.91721	2.44091	3.01901	3.67178	4.41902	5.28267
.12	1.12883	1.43336	1.93871	2.48415	3.09145	3.78203	4.57769	5.50226
.122	1.13064	1.44008	1.96025	2.52788	3.16542	3.89566	4.74243	5.73220
.124	1.13244	1.44674	1.98182	2.57209	3.24092	4.01269	4.91338	5.97259
.126	1.13423	1.45334	2.00342	2.61677	3.31795	4.13315	5.09067	6.22353
.128	1.13601	1.45988	2.02506	2.66193	3.39650	4.25704	5.27448	6.48508
.13	1.13778	1.46637	2.04673	2.70756	3.47657	4.38437	5.46489	6.75730
.132	1.13954	1.47279	2.06839	2.75358	3.55800	4.51503	5.66192	7.04178
.134	1.14129	1.47914	2.09002	2.79997	3.60479	4.64898	5.86561	7.33871
.136	1.14303	1.48541	2.11162	2.84672	3.72493	4.78619	6.07598	7.64814
.138	1.15576	1.49159	2.13319	2.89383	3.81042	4.92664	6.29305	7.97012
.14	1.14648	1.49769	2.15471	2.94130	3.89726	5.07033	6.51684	8.30480
.142	1.14819	1.50373	2.17618	2.98905	3.98528	5.21723	6.74738	8.65223
.144	1.14989	1.50970	2.19760	3.03705	4.07448	5.36732	6.98470	9.01246
.146	1.15158	1.51560	2.21896	3.08529	4.16485	5.52058	7.22884	9.38552
.148	1.15326	1.52148	2.24027	3.13375	4.25639	5.67698	7.47988	9.77144
.15	1.15493	1.52718	2.26151	3.18243	4.34908	5.83648	7.73785	10.17028
.152	1.15659	1.53285	2.28264	3.23125	4.44268	5.99888	8.00262	10.58227
.154	1.15824	1.53844	2.30366	3.28019	4.53717	6.16400	8.27371	11.00754
.156	1.15988	1.54395	2.32456	3.32925	4.63255	6.33179	8.55085	11.44613
.158	1.16151	1.54939	2.34534	3.37842	4.72881	6.50215	8.83389	11.89795
.16	1.16313	1.55475	2.36601	3.42769	4.82594	6.67493	9.12281	12.36275
.162	1.16474	1.56003	2.38654	3.47706	4.92364	6.85006	9.41760	12.84008
.164	1.16634	1.56523	2.40692	3.52635	5.02191	7.02747	9.71825	13.32964
.166	1.16793	1.57034	2.42714	3.57553	5.12075	7.20709	10.02475	13.83108

NACA

TABLE 2.- $Y_{-k}(\tau)$ FOR VARIOUS VALUES OF k - Concluded

τ	Y_{-9}	Y_{-10}	Y_{-11}	Y_{-12}	Y_{-13}	Y_{-14}	Y_{-15}
0.02	1.26173	1.29433	1.32780	1.36215	1.39740	1.43358	1.47069
.022	1.29254	1.32938	1.36725	1.40656	1.44631	1.48790	1.53051
.024	1.32433	1.36562	1.40820	1.45257	1.49742	1.54464	1.59303
.026	1.35717	1.40314	1.45073	1.50035	1.55083	1.60393	1.65845
.028	1.39111	1.44203	1.49492	1.55000	1.60665	1.66592	1.72707
.03	1.42621	1.48239	1.54087	1.60171	1.66500	1.73081	1.79925
.032	1.46251	1.52422	1.58861	1.65556	1.72590	1.79870	1.87504
.034	1.50005	1.56755	1.63815	1.71164	1.78938	1.86969	1.95450
.036	1.53885	1.61239	1.68951	1.77005	1.85547	1.94388	2.03772
.038	1.57893	1.65876	1.74275	1.83089	1.92425	2.02147	2.12480
.04	1.62030	1.70668	1.79793	1.89423	1.99580	2.10292	2.21584
.042	1.66317	1.75636	1.85530	1.96028	2.07055	2.18835	2.31150
.044	1.70769	1.80807	1.91511	2.02918	2.14895	2.27790	2.41226
.046	1.75396	1.86206	1.97760	2.10108	2.23129	2.37171	2.51052
.048	1.80208	1.91838	2.04292	2.17618	2.31780	2.47003	2.63068
.05	1.85215	1.97710	2.11119	2.25487	2.40866	2.57318	2.74913
.052	1.90423	2.03825	2.18244	2.33720	2.50391	2.68143	2.87396
.054	1.95838	2.10187	2.25671	2.42324	2.60360	2.79518	3.00527
.056	2.01466	2.16801	2.33404	2.51308	2.70778	2.91488	3.14317
.058	2.07311	2.23671	2.41448	2.60687	2.81652	3.04108	3.28785
.06	2.13375	2.30801	2.49811	2.70506	2.93004	3.17438	3.43959
.062	2.19706	2.38245	2.58554	2.80805	3.04926	3.31493	3.59973
.064	2.26332	2.46052	2.67742	2.91624	3.17508	3.46293	3.76947
.066	2.33293	2.54284	2.77440	3.03003	3.30840	3.61858	3.95001
.068	2.40612	2.62966	2.87683	3.14994	3.44952	3.78223	4.14215
.07	2.48306	2.72111	2.98490	3.27669	3.59897	3.95453	4.34650
.072	2.56380	2.81742	3.09865	3.41038	3.75686	4.13668	4.56329
.074	2.64845	2.91826	3.21816	3.55117	3.92331	4.32988	4.79276
.076	2.73708	3.02385	3.34351	3.69935	4.09845	4.53533	5.03516
.078	2.82975	3.13424	3.47478	3.85523	4.28249	4.75423	5.29096
.08	2.92651	3.24946	3.61220	4.01938	4.47610	4.98795	5.56117
.082	3.02836	3.37108	3.75702	4.19323	4.68161	5.23689	5.84888
.084	3.13620	3.50044	3.91154	4.37808	4.90102	5.50145	6.15759
.086	3.25074	3.63862	4.07696	4.57533	5.13623	5.78211	6.48930
.088	3.37247	3.78585	4.25398	4.78634	5.38854	6.07977	6.84676
.09	3.50151	3.94256	4.44325	5.01237	5.65958	6.39561	7.23250
.092	3.63790	4.10883	4.64479	5.25372	5.94962	6.73313	7.64714
.094	3.78172	4.28475	4.85862	5.51072	6.25906	7.09663	8.09158
.096	3.93303	4.47042	5.08476	5.78372	6.58820	7.49023	8.56682
.098	4.09187	4.66595	5.32323	6.07332	6.93844	7.91703	9.07396
.10	4.25830	4.87150	5.57405	6.38120	7.31014	8.38040	9.61427
.102	4.43508	5.09076	5.84187	6.71070	7.70884	8.88127	10.19878
.104	4.62319	5.32552	6.13119	7.06590	8.14254	9.42059	10.83739
.106	4.82310	5.57698	6.44401	7.45100	8.61424	9.99946	11.53600
.108	5.03533	5.84589	6.78133	7.86760	9.12794	10.61918	12.30271
.11	5.26038	6.13305	7.14387	8.31833	9.68601	11.28133	13.14450
.112	5.49838	6.43861	7.53176	8.80346	10.28948	11.99768	14.06339
.114	5.74949	6.76277	7.94513	9.32329	10.93955	12.78323	15.06158
.116	6.01384	7.10583	8.38415	9.87817	11.63752	13.64888	16.14137
.118	6.29157	7.46827	8.84967	10.46975	12.38489	14.60153	17.30516
.12	6.58282	7.85083	9.34325	11.10378	13.18426	15.64628	18.56319
.122	6.89106	8.25760	9.87193	11.78681	14.05003	16.78463	19.94042
.124	7.21718	8.69158	10.44041	12.52584	14.99560	18.01818	21.46378
.126	7.56168	9.15477	11.05289	13.32487	16.02797	19.34863	23.14824
.128	7.92507	9.64800	11.71096	14.18790	17.15434	20.77808	25.00800
.13	8.30784	10.17177	12.41548	15.11898	18.37894	22.31221	27.06023
.132	8.71012	10.72621	13.16665	16.11916	19.70334	23.98144	29.31086
.134	9.13204	11.31158	13.96467	17.18957	21.12914	25.81577	31.76599
.136	9.57373	11.92815	14.80979	18.33166	22.65874	27.83710	34.43182
.138	10.03536	12.57622	15.70291	19.54880	24.29334	30.05143	37.31415
.14	10.51724	13.25610	16.65687	20.84427	26.03917	32.46717	40.41914
.142	11.02162	13.97525	17.65183	22.23274	27.91600	35.08651	43.80673
.144	11.54950	14.73467	18.72179	23.72121	29.95183	37.91165	47.53692
.146	12.10178	15.53486	19.85925	25.31368	32.15966	40.94479	51.64171
.148	12.67906	16.37632	21.06551	27.01415	34.54349	44.18893	56.15450
.15	13.28171	17.25956	22.34143	28.82866	37.10348	47.65058	61.08451
.152	13.90826	18.18465	23.68721	30.75737	39.84047	51.41098	66.43272
.154	14.55831	19.15174	25.10315	32.80058	42.75546	55.47628	72.20013
.156	15.23156	20.16105	26.58955	34.95859	45.84945	59.86098	78.38754
.158	15.92794	21.21293	28.14695	37.23170	49.12444	64.57768	84.99595
.16	16.64743	22.30764	29.77649	39.62098	52.58311	69.63353	92.04144
.162	17.39220	23.44645	31.48333	42.13236	56.24378	75.03118	99.65693
.164	18.16212	24.63017	33.27307	44.77714	60.12845	80.77293	107.88242
.166	18.95704	25.86010	35.14681	47.56782	64.26012	86.86158	116.73291

NACA

TABLE 3.- $Y_k'(\tau)$ FOR VARIOUS VALUES OF k

τ	Y_1'	Y_2'	Y_3'	Y_4'	Y_5'	Y_6'	Y_7'	Y_8'
0.02	-1.225	-2.413	-3.551	-4.6345	-5.664	-6.640	-7.565	-8.440
.022	-1.222	-2.404	-3.531	-4.599	-5.608	-6.558	-7.454	-8.295
.024	-1.219	-2.396	-3.511	-4.564	-5.552	-6.477	-7.344	-8.152
.026	-1.217	-2.387	-3.493	-4.529	-5.497	-6.397	-7.236	-8.012
.028	-1.215	-2.379	-3.473	-4.494	-5.442	-6.318	-7.129	-7.874
.03	-1.213	-2.370	-3.454	-4.459	-5.387	-6.240	-7.023	-7.738
.032	-1.210	-2.362	-3.435	-4.424	-5.333	-6.162	-6.918	-7.604
.034	-1.207	-2.353	-3.416	-4.390	-5.279	-6.085	-6.814	-7.472
.036	-1.204	-2.345	-3.397	-4.356	-5.225	-6.009	-6.712	-7.341
.038	-1.202	-2.336	-3.378	-4.322	-5.172	-5.934	-6.611	-7.212
.04	-1.200	-2.328	-3.359	-4.288	-5.119	-5.859	-6.512	-7.084
.042	-1.197	-2.319	-3.340	-4.2545	-5.067	-5.785	-6.414	-6.958
.044	-1.194	-2.311	-3.321	-4.221	-5.015	-5.712	-6.317	-6.834
.046	-1.192	-2.302	-3.302	-4.1875	-4.964	-5.639	-6.221	-6.712
.048	-1.190	-2.294	-3.283	-4.1545	-4.913	-5.567	-6.125	-6.593
.05	-1.188	-2.286	-3.265	-4.1215	-4.862	-5.495	-6.030	-6.476
.052	-1.185	-2.277	-3.246	-4.089	-4.812	-5.424	-5.936	-6.360
.054	-1.182	-2.269	-3.227	-4.0565	-4.762	-5.354	-5.844	-6.246
.056	-1.180	-2.260	-3.208	-4.024	-4.712	-5.285	-5.754	-6.133
.058	-1.178	-2.252	-3.190	-3.9915	-4.663	-5.217	-5.665	-6.021
.06	-1.176	-2.244	-3.172	-3.9595	-4.614	-5.150	-5.577	-5.911
.062	-1.173	-2.235	-3.154	-3.9275	-4.566	-5.083	-5.490	-5.803
.064	-1.170	-2.227	-3.136	-3.896	-4.518	-5.017	-5.404	-5.696
.066	-1.168	-2.218	-3.118	-3.8645	-4.470	-4.951	-5.319	-5.591
.068	-1.166	-2.210	-3.100	-3.833	-4.423	-4.885	-5.235	-5.488
.07	-1.164	-2.203	-3.082	-3.8015	-4.376	-4.820	-5.152	-5.387
.072	-1.161	-2.195	-3.064	-3.7705	-4.329	-4.756	-5.070	-5.287
.074	-1.158	-2.186	-3.046	-3.7395	-4.283	-4.693	-4.990	-5.189
.076	-1.156	-2.178	-3.028	-3.7085	-4.237	-4.631	-4.910	-5.092
.078	-1.154	-2.170	-3.010	-3.678	-4.191	-4.569	-4.831	-4.996
.08	-1.152	-2.162	-2.993	-3.6485	-4.146	-4.508	-4.753	-4.901
.082	-1.149	-2.154	-2.975	-3.6185	-4.101	-4.448	-4.676	-4.807
.084	-1.146	-2.146	-2.957	-3.5885	-4.057	-4.388	-4.600	-4.715
.086	-1.143	-2.138	-2.940	-3.5585	-4.013	-4.329	-4.525	-4.625
.088	-1.141	-2.130	-2.923	-3.5285	-3.969	-4.270	-4.451	-4.537
.09	-1.139	-2.122	-2.906	-3.4995	-3.926	-4.211	-4.378	-4.451
.092	-1.136	-2.114	-2.888	-3.4705	-3.883	-4.153	-4.306	-4.366
.094	-1.133	-2.106	-2.871	-3.4415	-3.840	-4.096	-4.235	-4.282
.096	-1.131	-2.098	-2.854	-3.4125	-3.798	-4.040	-4.165	-4.199
.098	-1.129	-2.090	-2.837	-3.3835	-3.756	-3.984	-4.096	-4.117
.10	-1.127	-2.082	-2.820	-3.3545	-3.714	-3.929	-4.028	-4.035
.102	-1.124	-2.074	-2.803	-3.326	-3.673	-3.875	-3.961	-3.955
.104	-1.121	-2.066	-2.787	-3.298	-3.632	-3.821	-3.895	-3.876
.106	-1.119	-2.058	-2.770	-3.270	-3.591	-3.768	-3.829	-3.799
.108	-1.117	-2.050	-2.753	-3.242	-3.551	-3.715	-3.764	-3.724
.11	-1.115	-2.042	-2.736	-3.214	-3.511	-3.662	-3.700	-3.651
.112	-1.112	-2.034	-2.720	-3.1865	-3.471	-3.610	-3.637	-3.579
.114	-1.109	-2.026	-2.703	-3.159	-3.432	-3.559	-3.575	-3.508
.116	-1.107	-2.018	-2.687	-3.1315	-3.393	-3.508	-3.513	-3.437
.118	-1.105	-2.010	-2.670	-3.1045	-3.354	-3.458	-3.452	-3.367
.12	-1.103	-2.003	-2.654	-3.0775	-3.316	-3.409	-3.392	-3.297
.122	-1.100	-1.995	-2.637	-3.051	-3.278	-3.360	-3.333	-3.228
.124	-1.098	-1.987	-2.620	-3.0245	-3.240	-3.312	-3.275	-3.161
.126	-1.096	-1.979	-2.604	-2.998	-3.203	-3.264	-3.218	-3.096
.128	-1.094	-1.971	-2.588	-2.9715	-3.166	-3.216	-3.161	-3.033
.13	-1.092	-1.964	-2.572	-2.945	-3.129	-3.169	-3.105	-2.971
.132	-1.089	-1.956	-2.556	-2.919	-3.092	-3.122	-3.050	-2.910
.134	-1.086	-1.948	-2.540	-2.893	-3.056	-3.076	-2.996	-2.849
.136	-1.084	-1.940	-2.524	-2.867	-3.020	-3.031	-2.943	-2.789
.138	-1.082	-1.933	-2.508	-2.8415	-2.984	-2.986	-2.890	-2.730
.14	-1.080	-1.926	-2.493	-2.816	-2.949	-2.942	-2.838	-2.672
.142	-1.077	-1.918	-2.477	-2.7905	-2.914	-2.898	-2.786	-2.615
.144	-1.074	-1.910	-2.462	-2.7655	-2.879	-2.855	-2.735	-2.559
.146	-1.072	-1.902	-2.446	-2.7405	-2.845	-2.812	-2.685	-2.504
.148	-1.070	-1.895	-2.431	-2.716	-2.811	-2.770	-2.636	-2.450
.15	-1.068	-1.888	-2.415	-2.6915	-2.777	-2.728	-2.588	-2.397
.152	-1.065	-1.880	-2.400	-2.667	-2.743	-2.687	-2.541	-2.345
.154	-1.062	-1.872	-2.384	-2.6425	-2.710	-2.646	-2.495	-2.294
.156	-1.060	-1.864	-2.369	-2.6185	-2.677	-2.606	-2.449	-2.244
.158	-1.058	-1.857	-2.353	-2.5945	-2.644	-2.566	-2.403	-2.194
.16	-1.056	-1.850	-2.338	-2.5705	-2.612	-2.526	-2.358	-2.145
.162	-1.053	-1.842	-2.323	-2.547	-2.580	-2.487	-2.313	-2.097
.164	-1.050	-1.835	-2.308	-2.5235	-2.548	-2.448	-2.269	-2.050
.166	-1.048	-1.828	-2.293	-2.500	-2.517	-2.410	-2.226	-2.003

NACA

TABLE 3.- $Y_k'(\tau)$ FOR VARIOUS VALUES OF k - Concluded

τ	Y_9'	Y_{10}'	Y_{11}'	Y_{12}'	Y_{13}'	Y_{14}'	Y_{15}'
0.02	-9.266	-10.045	-10.780	-11.4705	-12.121	-12.731	-13.301
.022	-9.083	-9.824	-10.517	-11.161	-11.764	-12.324	-12.844
.024	-8.905	-9.607	-10.259	-10.859	-11.416	-11.929	-12.400
.026	-8.730	-9.394	-10.006	-10.564	-11.077	-11.545	-11.970
.028	-8.558	-9.185	-9.758	-10.277	-10.747	-11.172	-11.553
.03	-8.389	-8.980	-9.515	-9.996	-10.426	-10.810	-11.149
.032	-8.223	-8.779	-9.278	-9.722	-10.113	-10.458	-10.757
.034	-8.059	-8.582	-9.046	-9.454	-9.808	-10.116	-10.378
.036	-7.898	-8.388	-8.819	-9.192	-9.511	-9.784	-10.011
.038	-7.739	-8.198	-8.597	-8.936	-9.222	-9.462	-9.656
.04	-7.582	-8.012	-8.379	-8.6865	-8.942	-9.149	-9.313
.042	-7.428	-7.829	-8.166	-8.443	-8.669	-8.845	-8.981
.044	-7.277	-7.650	-7.958	-8.206	-8.403	-8.550	-8.659
.046	-7.129	-7.474	-7.754	-7.974	-8.144	-8.264	-8.346
.048	-6.983	-7.302	-7.555	-7.749	-7.892	-7.987	-8.043
.05	-6.841	-7.134	-7.360	-7.530	-7.647	-7.719	-7.749
.052	-6.699	-6.969	-7.169	-7.316	-7.409	-7.459	-7.464
.054	-6.560	-6.807	-6.983	-7.107	-7.178	-7.206	-7.189
.056	-6.424	-6.648	-6.801	-6.902	-6.953	-6.960	-6.924
.058	-6.290	-6.492	-6.623	-6.703	-6.734	-6.721	-6.670
.06	-6.160	-6.339	-6.449	-6.5085	-6.520	-6.489	-6.426
.062	-6.030	-6.189	-6.279	-6.319	-6.312	-6.264	-6.189
.064	-5.903	-6.042	-6.113	-6.134	-6.110	-6.046	-5.959
.066	-5.778	-5.898	-5.951	-5.954	-5.914	-5.835	-5.735
.068	-5.655	-5.757	-5.792	-5.779	-5.724	-5.632	-5.517
.07	-5.537	-5.620	-5.637	-5.6085	-5.540	-5.436	-5.304
.072	-5.417	-5.485	-5.485	-5.442	-5.360	-5.246	-5.098
.074	-5.301	-5.353	-5.337	-5.280	-5.185	-5.061	-4.891
.076	-5.187	-5.223	-5.193	-5.1225	-5.015	-4.881	-4.701
.078	-5.075	-5.095	-5.052	-4.969	-4.850	-4.706	-4.518
.08	-4.965	-4.970	-4.915	-4.8195	-4.690	-4.536	-4.361
.082	-4.857	-4.848	-4.781	-4.674	-4.535	-4.372	-4.189
.084	-4.751	-4.728	-4.650	-4.5315	-4.384	-4.214	-4.024
.086	-4.647	-4.610	-4.522	-4.393	-4.237	-4.061	-3.866
.088	-4.545	-4.495	-4.397	-4.258	-4.095	-3.913	-3.714
.09	-4.444	-4.383	-4.273	-4.1265	-3.957	-3.770	-3.570
.092	-4.345	-4.273	-4.154	-3.999	-3.823	-3.632	-3.430
.094	-4.248	-4.165	-4.037	-3.874	-3.693	-3.498	-3.294
.096	-4.153	-4.059	-3.923	-3.753	-3.567	-3.368	-3.162
.098	-4.060	-3.956	-3.812	-3.636	-3.444	-3.242	-3.033
.10	-3.969	-3.855	-3.705	-3.522	-3.325	-3.119	-2.908
.102	-3.879	-3.757	-3.600	-3.411	-3.210	-3.001	-2.788
.104	-3.791	-3.660	-3.497	-3.303	-3.098	-2.887	-2.673
.106	-3.705	-3.565	-3.396	-3.198	-2.989	-2.777	-2.563
.108	-3.620	-3.473	-3.297	-3.095	-2.884	-2.671	-2.458
.11	-3.538	-3.383	-3.201	-2.9955	-2.782	-2.569	-2.357
.112	-3.455	-3.294	-3.107	-2.8985	-2.684	-2.470	-2.259
.114	-3.375	-3.207	-3.016	-2.804	-2.589	-2.374	-2.164
.116	-3.297	-3.122	-2.927	-2.712	-2.496	-2.281	-2.072
.118	-3.220	-3.039	-2.840	-2.623	-2.406	-2.191	-1.984
.12	-3.145	-2.959	-2.755	-2.5365	-2.319	-2.105	-1.899
.122	-3.072	-2.879	-2.672	-2.452	-2.235	-2.022	-1.817
.124	-3.000	-2.801	-2.591	-2.372	-2.153	-1.942	-1.738
.126	-2.929	-2.725	-2.512	-2.293	-2.074	-1.864	-1.663
.128	-2.859	-2.651	-2.436	-2.216	-1.997	-1.789	-1.591
.13	-2.790	-2.581	-2.362	-2.1405	-1.922	-1.717	-1.522
.132	-2.723	-2.509	-2.289	-2.068	-1.850	-1.647	-1.455
.134	-2.658	-2.440	-2.218	-1.998	-1.781	-1.580	-1.391
.136	-2.594	-2.372	-2.149	-1.9305	-1.714	-1.515	-1.329
.138	-2.531	-2.306	-2.082	-1.865	-1.650	-1.452	-1.270
.14	-2.469	-2.243	-2.017	-1.801	-1.588	-1.391	-1.213
.142	-2.409	-2.177	-1.953	-1.739	-1.527	-1.333	-1.158
.144	-2.350	-2.115	-1.891	-1.680	-1.468	-1.277	-1.105
.146	-2.292	-2.055	-1.831	-1.622	-1.411	-1.223	-1.054
.148	-2.235	-1.997	-1.773	-1.566	-1.356	-1.171	-1.005
.15	-2.176	-1.944	-1.716	-1.5115	-1.303	-1.122	-.958
.152	-2.124	-1.886	-1.661	-1.460	-1.252	-1.075	-.913
.154	-2.070	-1.832	-1.607	-1.411	-1.202	-1.029	-.870
.156	-2.018	-1.779	-1.555	-1.363	-1.154	-.984	-.829
.158	-1.967	-1.727	-1.504	-1.317	-1.108	-.940	-.790
.16	-1.917	-1.676	-1.455	-1.273	-1.063	-.898	-.753
.162	-1.868	-1.626	-1.407	-1.232	-1.020	-.858	-.718
.164	-1.820	-1.578	-1.360	-1.192	-.979	-.820	-.685
.166	-1.773	-1.531	-1.315	-1.155	-.939	-.783	-.654

NACA

TABLE 4.- $Y_{-k}'(\tau)$ FOR VARIOUS VALUES OF k

τ	Y_{-1}'	Y_{-2}'	Y_{-3}'	Y_{-4}'	Y_{-5}'	Y_{-6}'	Y_{-7}'	Y_{-8}'
0.02	1.188	3.418	5.055	6.399	7.895	9.546	11.319	13.197
.022	1.182	3.476	5.210	6.589	8.108	9.805	11.631	13.590
.024	1.176	3.525	5.367	6.788	8.334	10.075	11.960	14.000
.026	1.170	3.569	5.525	6.996	8.574	10.358	12.307	14.428
.028	1.164	3.610	5.684	7.213	8.828	10.656	12.672	14.875
.03	1.158	3.638	5.844	7.439	9.097	10.969	13.056	15.342
.032	1.152	3.673	6.005	7.676	9.381	11.299	13.459	15.831
.034	1.146	3.704	6.166	7.922	9.679	11.648	13.882	16.344
.036	1.140	3.732	6.327	8.175	9.992	12.018	14.326	16.883
.038	1.134	3.757	6.488	8.437	10.320	12.410	14.792	17.451
.04	1.129	3.779	6.648	8.707	10.664	12.825	15.281	18.050
.042	1.123	3.799	6.807	8.985	11.025	13.263	15.798	18.682
.044	1.117	3.817	6.965	9.271	11.405	13.725	16.347	19.349
.046	1.111	3.833	7.122	9.564	11.803	14.212	16.932	20.054
.048	1.105	3.847	7.277	9.864	12.219	14.726	17.554	20.799
.05	1.100	3.859	7.432	10.172	12.653	15.268	18.215	21.587
.052	1.094	3.869	7.583	10.486	13.106	15.839	18.915	22.423
.054	1.088	3.877	7.732	10.806	13.576	16.441	19.655	23.312
.056	1.082	3.883	7.879	11.131	14.064	17.076	20.438	24.259
.058	1.076	3.887	8.025	11.461	14.570	17.745	21.265	25.268
.06	1.071	3.889	8.170	11.795	15.094	18.449	22.138	26.342
.062	1.065	3.889	8.312	12.134	15.636	19.187	23.066	27.485
.064	1.059	3.888	8.450	12.477	16.196	19.960	24.051	28.701
.066	1.053	3.886	8.584	12.824	16.773	20.768	25.095	29.994
.068	1.048	3.883	8.714	13.173	17.368	21.612	26.196	31.369
.07	1.043	3.878	8.841	13.524	17.979	22.494	27.360	32.829
.072	1.037	3.872	8.965	13.877	18.606	23.413	28.588	34.384
.074	1.031	3.864	9.086	14.232	19.249	24.370	29.882	36.039
.076	1.025	3.854	9.204	14.588	19.907	25.366	31.245	37.800
.078	1.020	3.843	9.319	14.944	20.581	26.403	32.679	39.673
.08	1.015	3.831	9.430	15.301	21.270	27.482	34.186	41.662
.082	1.009	3.818	9.537	15.658	21.973	28.601	35.768	43.770
.084	1.003	3.804	9.640	16.013	22.688	29.758	37.426	46.002
.086	.997	3.789	9.739	16.367	23.413	30.950	39.162	48.363
.088	.992	3.772	9.834	16.719	24.148	32.175	40.976	50.858
.09	.987	3.754	9.924	17.069	24.892	33.430	42.870	53.492
.092	.981	3.736	10.010	17.416	25.646	34.724	44.844	56.270
.094	.975	3.718	10.092	17.760	26.409	36.056	46.900	59.198
.096	.970	3.699	10.170	18.100	27.180	37.426	49.039	62.280
.098	.965	3.670	10.244	18.436	27.959	38.834	51.260	65.520
.10	.960	3.651	10.315	18.768	28.746	40.280	53.563	68.919
.102	.954	3.628	10.381	19.095	29.538	41.752	55.947	72.480
.104	.949	3.604	10.442	19.416	30.330	43.249	58.411	76.205
.106	.944	3.579	10.498	19.732	31.122	44.771	60.954	80.096
.108	.939	3.553	10.549	20.041	32.914	46.318	63.575	84.154
.11	.934	3.525	10.596	20.342	32.706	47.891	66.272	88.378
.112	.928	3.497	10.639	20.636	33.498	49.484	69.044	92.770
.114	.923	3.468	10.677	20.923	34.288	51.096	71.889	97.331
.116	.918	3.439	10.711	21.203	35.074	52.727	74.803	102.062
.118	.913	3.410	10.740	21.475	35.854	54.377	77.781	106.960
.12	.908	3.380	10.765	21.737	36.627	56.044	80.820	112.021
.122	.902	3.349	10.785	21.990	37.392	57.724	83.917	117.241
.124	.897	3.317	10.801	22.233	38.148	59.411	87.069	122.615
.126	.892	3.285	10.812	22.466	38.893	61.097	90.273	128.137
.128	.887	3.252	10.818	22.689	39.628	62.773	93.524	133.799
.13	.882	3.219	10.819	22.903	40.351	64.436	96.817	139.595
.132	.877	3.185	10.815	23.106	41.060	66.076	100.146	145.520
.134	.872	3.150	10.808	23.297	41.752	67.753	103.503	151.568
.136	.867	3.115	10.796	23.476	42.426	69.407	106.879	157.731
.138	.862	3.079	10.779	23.642	43.080	71.058	110.265	163.991
.14	.857	3.043	10.758	23.796	43.714	72.698	113.647	170.340
.142	.852	3.007	10.732	23.937	44.327	74.298	117.029	176.767
.144	.847	2.970	10.701	24.066	44.918	75.873	120.407	183.258
.146	.842	2.933	10.666	24.182	45.486	77.403	123.777	189.794
.148	.837	2.895	10.627	24.286	46.030	78.910	127.134	196.353
.15	.833	2.856	10.584	24.377	46.549	80.402	130.473	202.915
.152	.828	2.817	10.537	24.454	47.041	81.844	133.784	209.468
.154	.823	2.778	10.485	24.516	47.503	83.233	137.051	215.999
.156	.818	2.738	10.428	24.563	47.933	84.568	140.248	222.504
.158	.813	2.698	10.366	24.596	48.330	85.848	143.333	228.965
.16	.808	2.658	10.298	24.614	48.694	87.076	146.247	235.362
.162	.803	2.618	10.225	24.617	49.024	88.244	148.925	241.671
.164	.798	2.777	10.147	24.605	49.319	89.346	151.298	247.862
.166	.793	2.736	10.064	24.577	49.579	90.376	153.271	253.899

NACA

TABLE 4.- $Y_{-k}'(\tau)$ FOR VARIOUS VALUES OF k - Concluded

τ	Y_{-9}'	Y_{-10}'	Y_{-11}'	Y_{-12}'	Y_{-13}'	Y_{-14}'	Y_{-15}'
0.02	15.174	17.250	19.426	21.706	24.092	26.588	29.199
.022	15.656	17.833	20.146	22.562	25.104	27.768	30.564
.024	16.160	18.451	20.896	23.455	26.162	29.010	32.008
.026	16.688	19.096	21.680	24.388	27.270	30.317	33.535
.028	17.240	19.772	22.488	25.365	28.433	31.692	35.149
.03	17.817	20.479	23.335	26.390	29.655	33.140	36.855
.032	18.420	21.219	24.230	27.467	30.941	34.666	38.658
.034	19.051	21.992	25.168	28.599	32.296	36.276	40.563
.036	19.712	22.800	26.153	29.790	33.724	37.975	42.567
.038	20.406	23.648	27.188	31.043	35.230	39.769	44.688
.04	21.135	24.540	28.277	32.362	36.818	41.666	46.935
.042	21.902	25.478	29.423	33.751	38.493	43.671	49.316
.044	22.711	26.466	30.630	35.215	40.260	45.791	51.841
.046	23.566	27.509	31.902	36.759	42.126	48.034	54.520
.048	24.471	28.611	33.244	38.390	44.099	50.409	57.364
.05	25.431	29.778	34.661	40.116	46.187	52.925	60.386
.052	26.447	31.013	36.161	41.943	48.408	55.595	63.598
.054	27.525	32.322	37.751	43.879	50.761	58.432	67.014
.056	28.670	33.711	39.440	45.934	53.256	61.450	70.651
.058	29.887	35.187	41.237	48.118	55.906	64.665	74.529
.06	31.184	36.760	43.152	50.444	58.724	68.096	78.673
.062	32.567	38.437	45.194	52.924	61.729	71.758	83.098
.064	34.043	40.228	47.374	55.572	64.941	75.669	87.830
.066	35.621	42.144	49.704	58.404	68.382	79.852	92.899
.068	37.309	44.198	52.198	61.437	72.076	84.332	98.339
.07	39.114	46.402	54.869	64.690	76.047	89.140	104.190
.072	41.045	48.762	57.738	68.186	80.315	94.308	110.484
.074	43.110	51.294	60.826	71.949	84.906	99.880	117.268
.076	45.317	54.014	64.155	76.008	89.852	105.903	124.597
.078	47.675	56.938	67.747	80.394	95.192	112.426	132.533
.08	50.196	60.084	71.626	85.142	100.974	119.502	141.148
.082	52.891	63.465	75.815	90.284	107.246	127.190	150.506
.084	55.772	67.099	80.338	95.854	114.061	135.551	160.691
.086	58.850	71.005	85.220	101.888	121.475	144.648	171.798
.088	62.136	75.202	90.487	108.436	129.548	154.548	183.934
.09	65.640	79.712	96.165	115.514	138.343	165.321	197.218
.092	69.372	84.555	102.316	123.222	147.932	177.104	211.782
.094	73.342	89.752	108.970	131.602	158.401	190.036	227.786
.096	77.560	95.325	116.161	140.718	169.839	204.258	245.400
.098	82.035	101.295	123.925	150.636	182.340	219.921	264.814
.10	86.778	107.685	132.301	161.424	196.003	237.164	286.239
.102	91.806	114.515	141.331	173.143	210.936	256.114	309.879
.104	97.123	121.809	151.056	185.856	227.249	276.014	335.979
.106	102.738	129.589	161.519	199.629	245.062	299.714	364.809
.108	108.660	137.876	172.764	214.533	264.506	324.685	396.668
.11	114.895	146.690	184.834	230.644	285.722	352.016	431.886
.112	121.454	156.050	197.776	248.082	308.854	382.094	470.796
.114	128.338	165.976	211.635	266.931	334.043	415.142	513.776
.116	135.551	176.486	226.452	287.276	361.439	451.412	561.236
.118	143.096	187.599	242.265	309.204	391.193	491.270	613.621
.12	150.976	199.331	259.112	332.805	423.459	534.809	671.426
.122	159.189	211.693	277.029	358.150	458.405	582.358	735.075
.124	167.732	224.693	296.057	385.312	496.195	634.187	805.018
.126	176.602	238.336	316.230	414.355	537.001	690.576	881.735
.128	185.796	252.624	337.583	445.355	580.986	751.804	965.736
.13	195.410	267.558	360.147	478.288	628.331	818.162	1057.568
.132	205.244	283.140	383.933	513.378	679.167	890.042	1157.823
.134	215.395	299.371	408.942	550.655	733.612	967.754	1267.107
.136	225.857	316.250	435.172	590.165	791.769	1051.578	1386.030
.138	236.620	333.776	462.619	631.947	853.717	1141.794	1515.182
.14	247.671	351.946	491.271	676.032	919.513	1238.671	1655.123
.142	258.965	370.695	521.138	722.387	989.282	1342.419	1806.364
.144	270.476	390.004	552.206	771.017	1063.136	1453.188	1969.214
.146	282.176	409.840	584.458	821.897	1141.196	1571.058	2143.873
.148	294.035	430.156	617.864	874.977	1223.595	1696.029	2330.341
.15	306.019	450.892	652.370	930.184	1310.520	1828.020	2528.419
.152	318.128	472.028	687.900	987.466	1400.675	1967.246	2740.02
.154	330.336	493.530	724.354	1046.750	1494.940	2113.795	2964.45
.156	342.614	515.359	761.608	1107.962	1593.145	2267.668	3201.92
.158	354.932	537.472	799.511	1171.003	1695.141	2428.965	3452.41
.16	367.256	559.821	837.885	1235.774	1800.767	2597.786	3715.74
.162	379.543	582.351	876.659	1302.046	1909.706	2773.500	3989.60
.164	391.731	604.991	915.777	1369.417	2021.549	2955.700	4273.90
.166	403.728	627.651	955.198	1437.259	2135.644	3143.500	4568.40

NACA

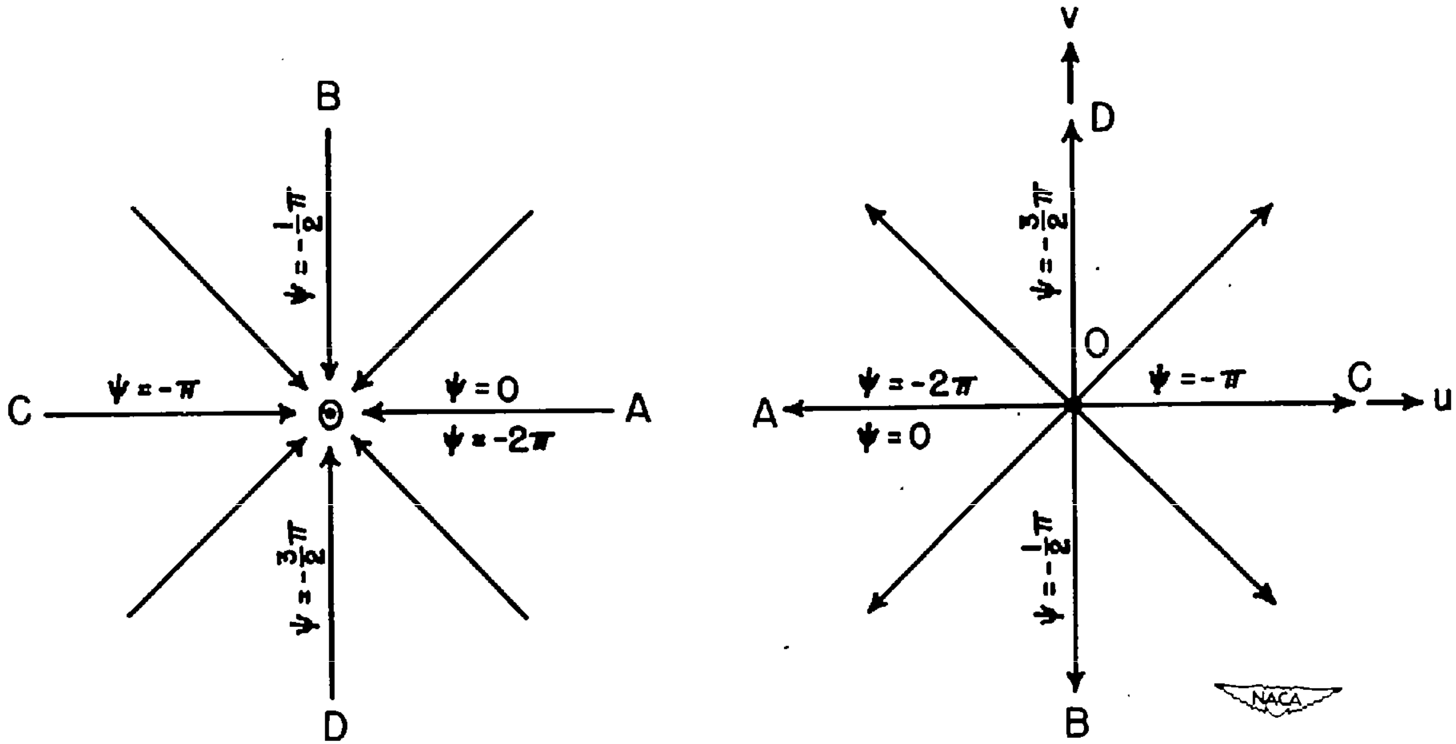

SINK

$w = \phi + i\psi = -\log_e z$

PHYSICAL PLANE

SOURCE

$w = \phi + i\psi = \log_e \bar{q}$

HODOGRAPH PLANE

(a) Incompressible flow.

Figure 1.- Sink (negative source) solution.

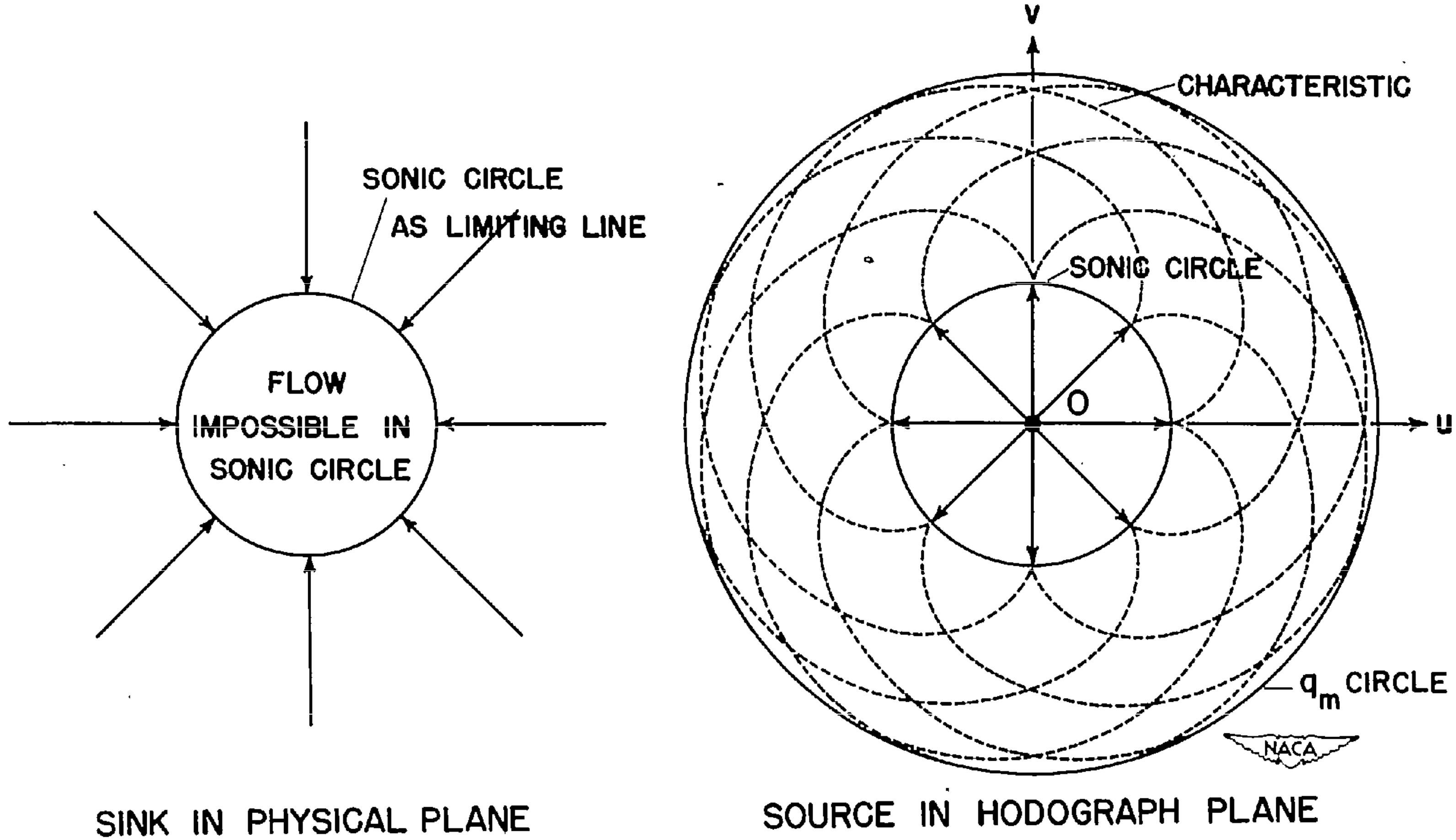

(b) Compressible flow.

Figure 1.- Concluded.

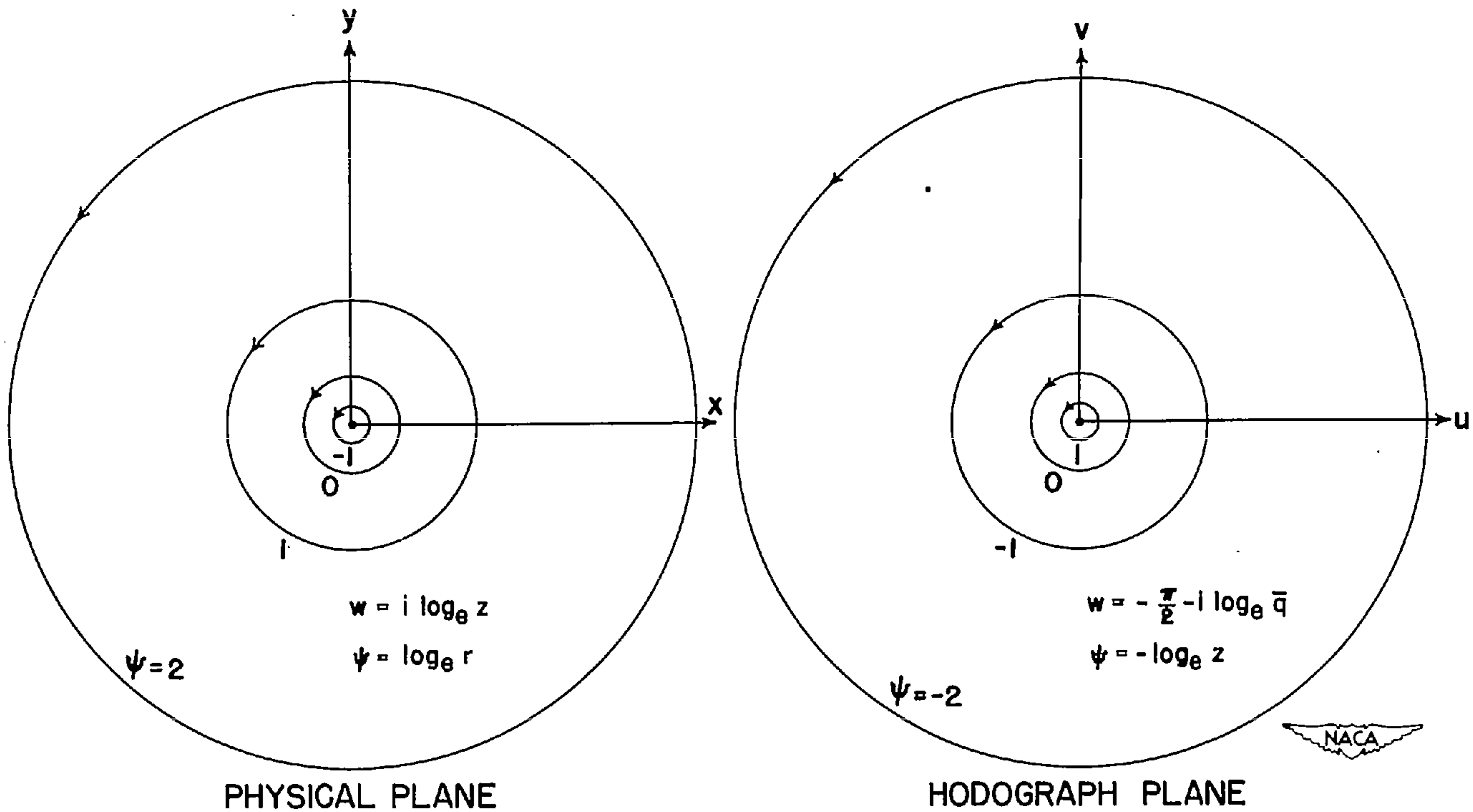

(a) Incompressible flow.

Figure 2.- Vortex in potential field.

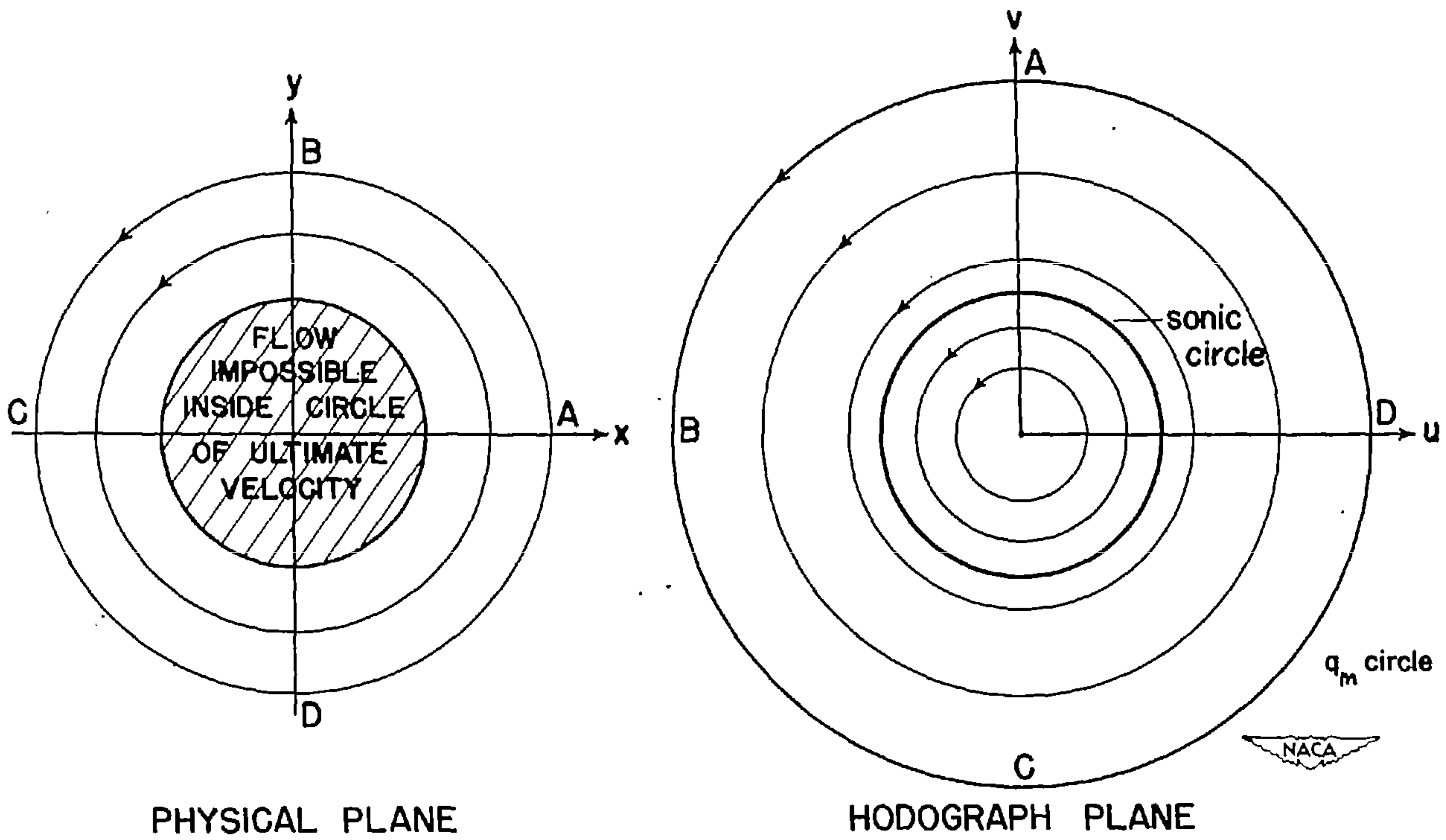

(b) Compressible flow.

Figure 2.- Concluded.

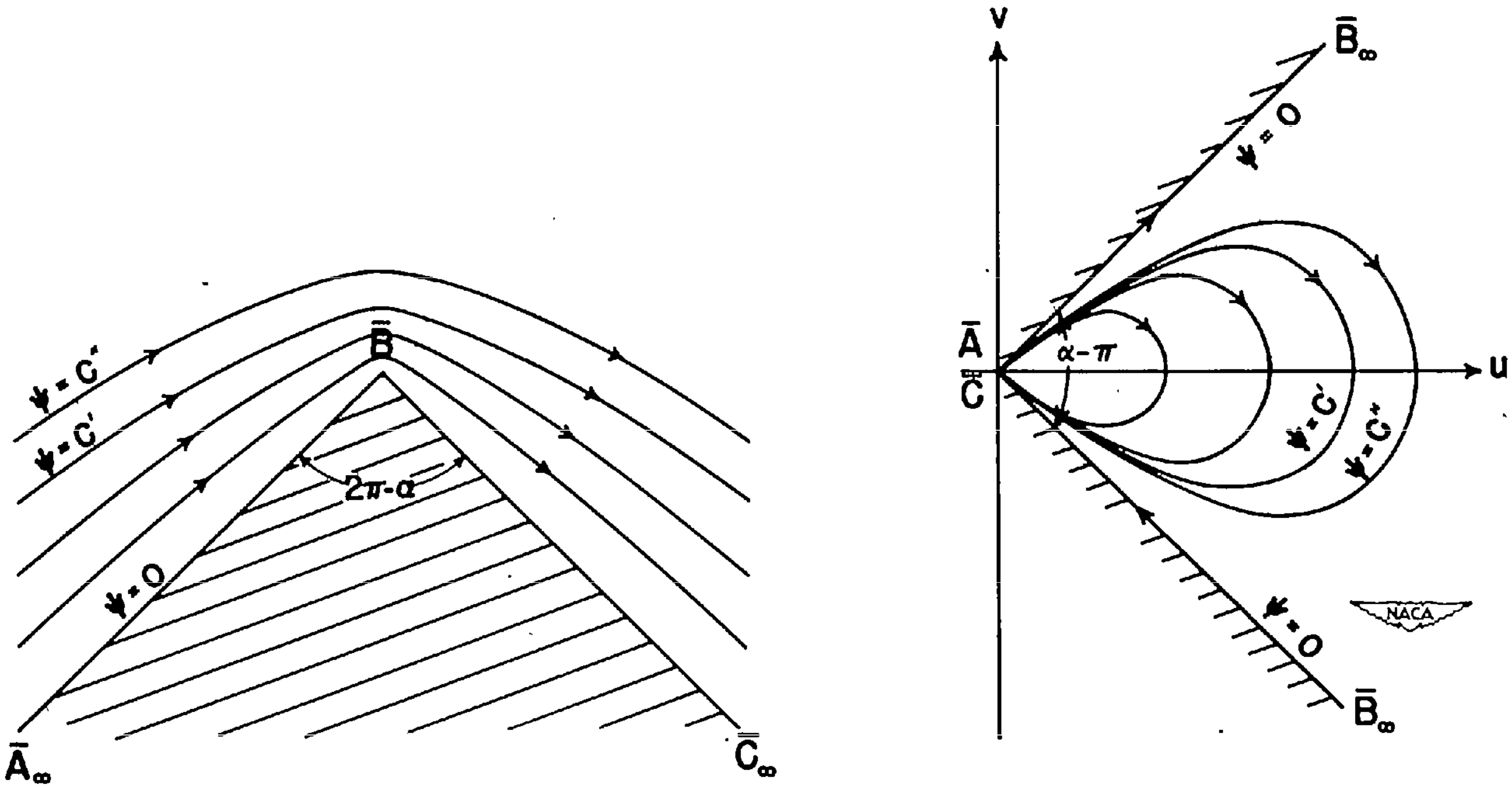

PHYSICAL PLANE HODOGRAPH PLANE

(a) Incompressible flow.

Figure 3.- Flow around a sharp convex corner (angle, 90°).

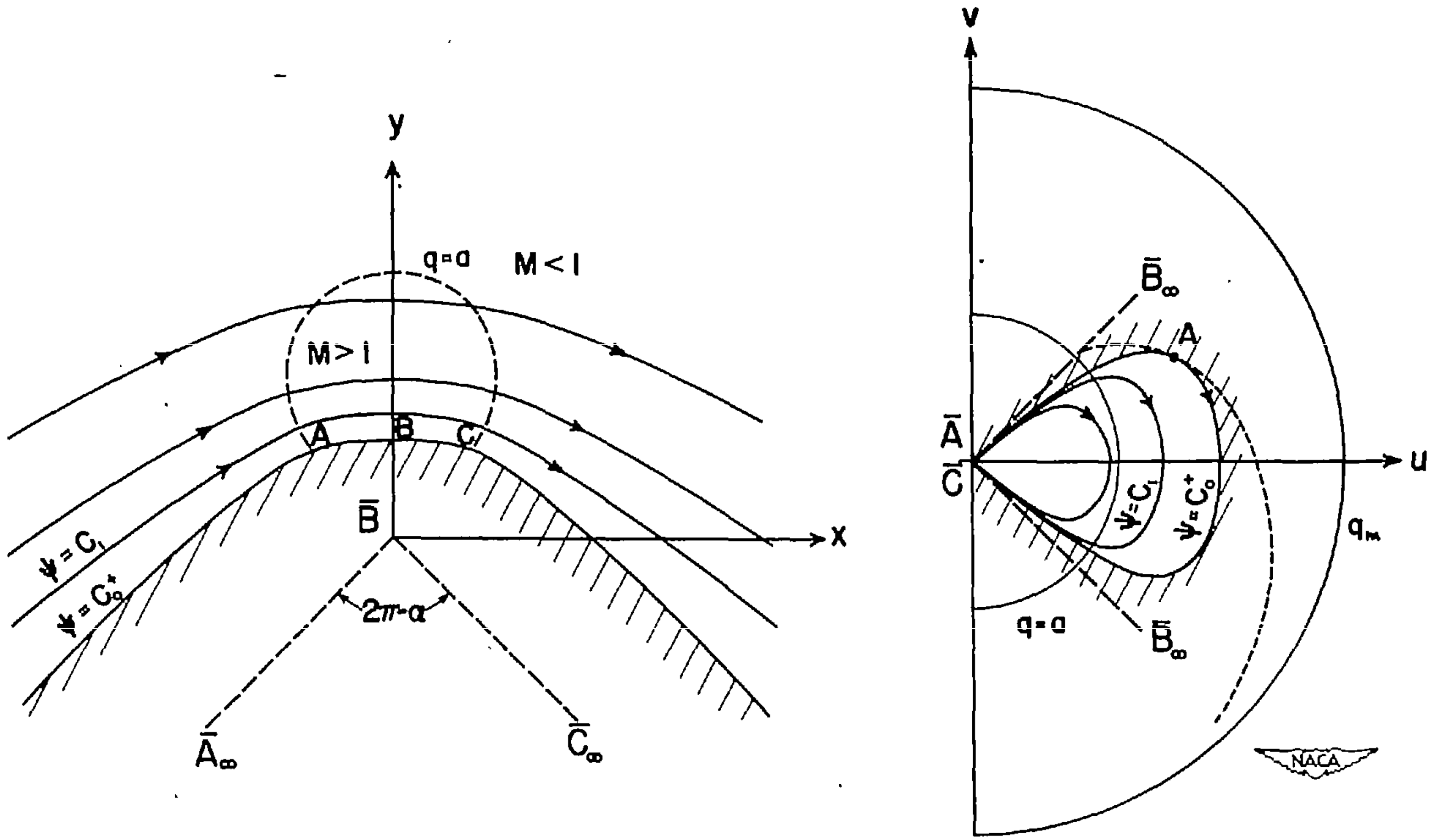

PHYSICAL PLANE

HODOGRAPH PLANE

(b) Compressible flow.

Figure 3.- Concluded.

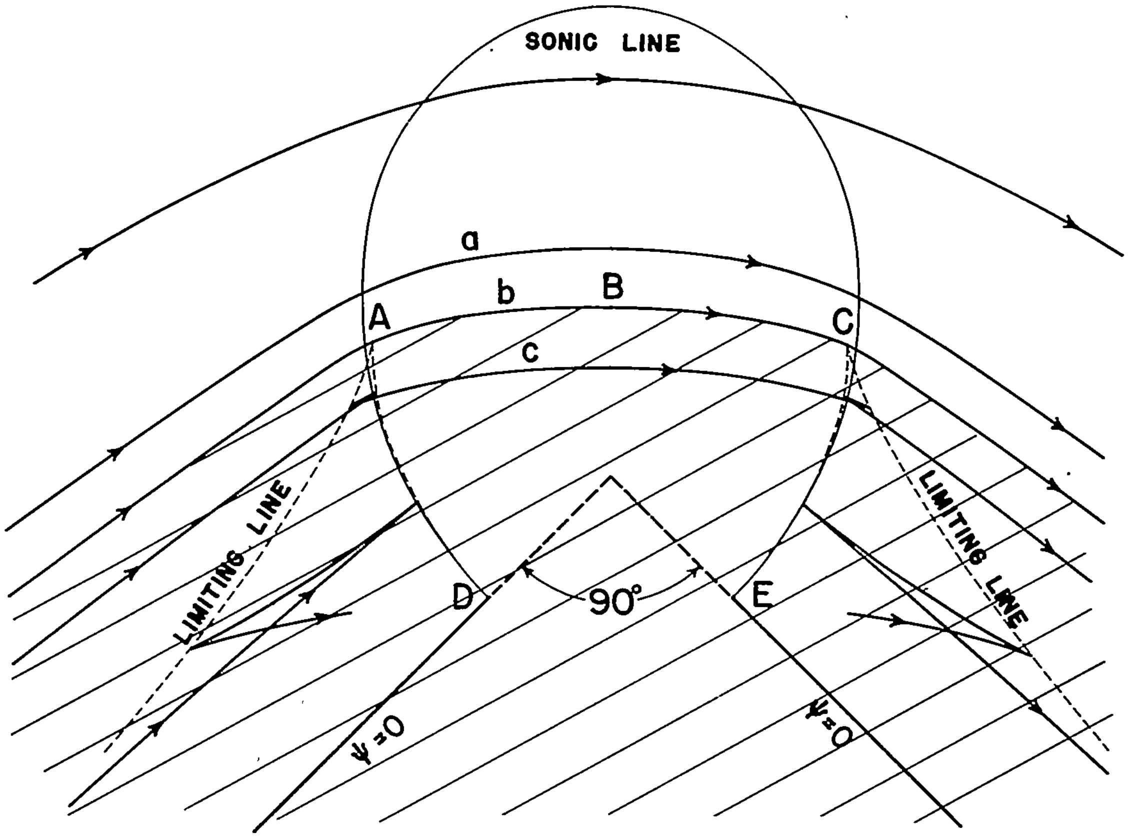

(a) Compressible flow streamlines.

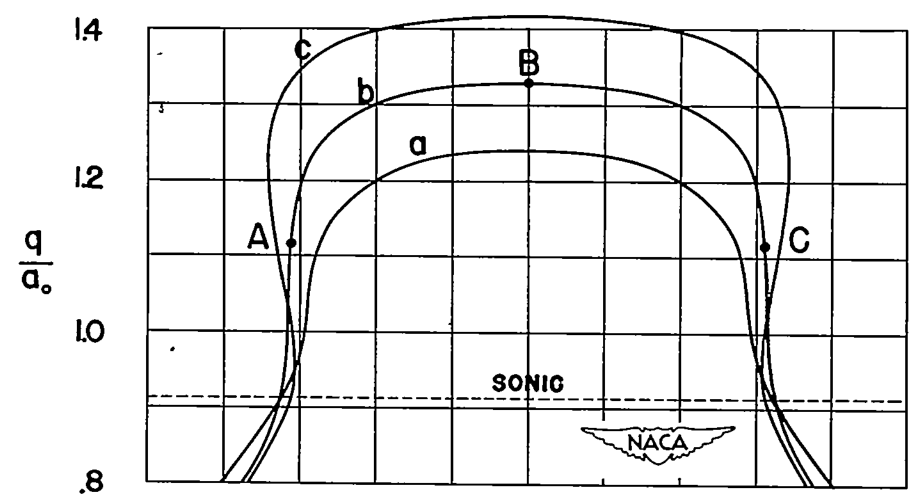

(b) Velocity distribution.

Figure 4.- Details of flow around a corner angle of 90°.

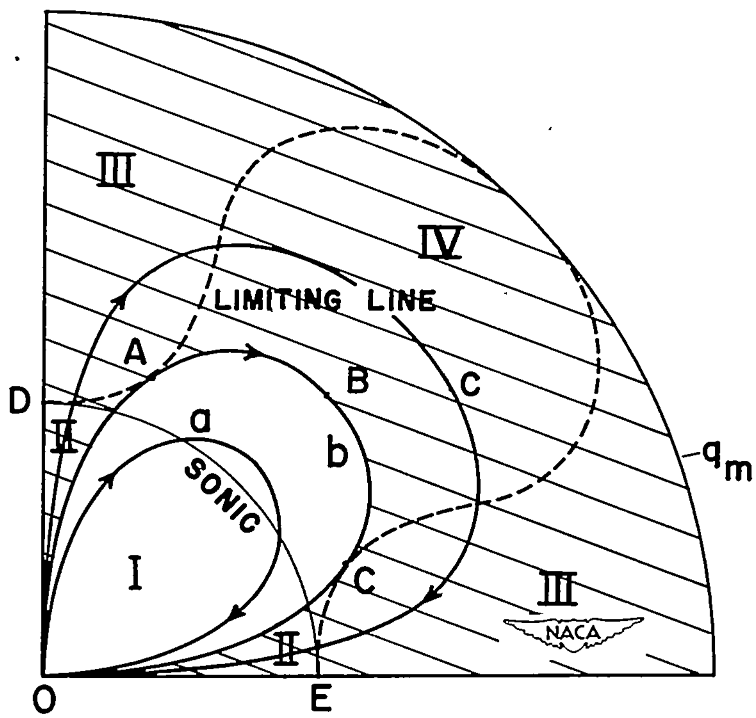

(c) Hodograph streamlines.

Figure 4.- Continued.

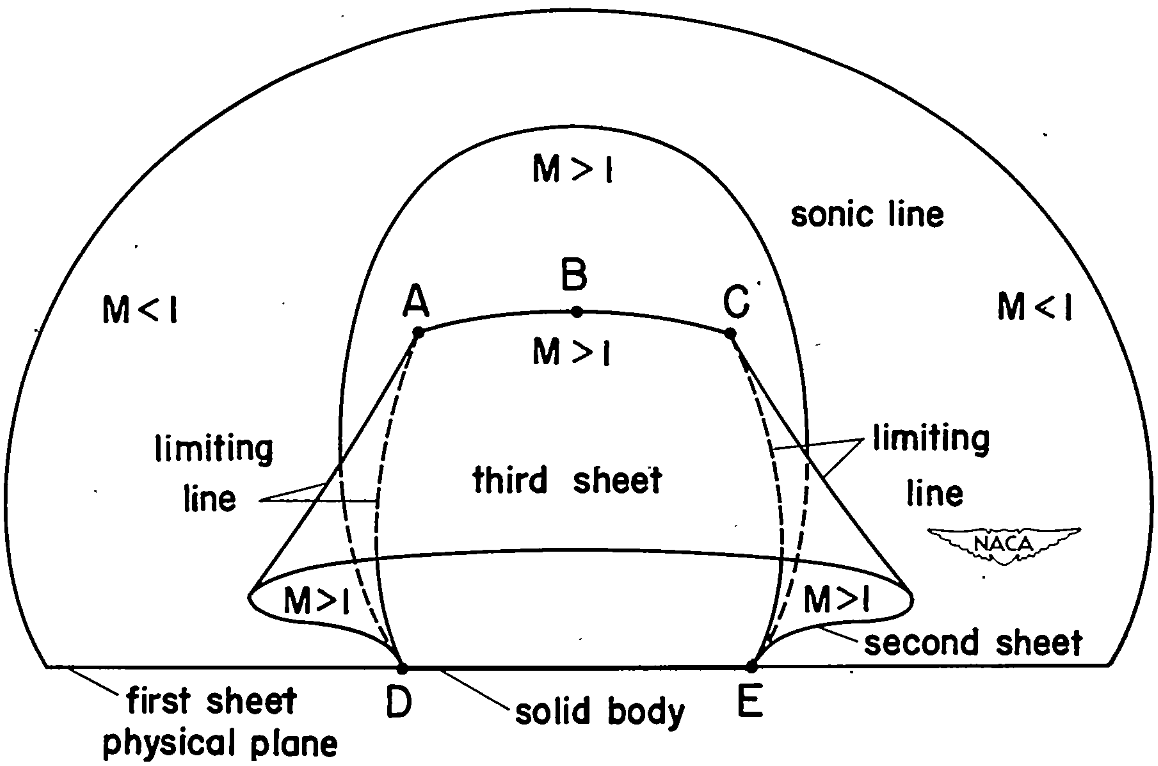

(d) Schematic view of multiple-sheeted Riemann surface in physical plane.

Figure 4.- Concluded.

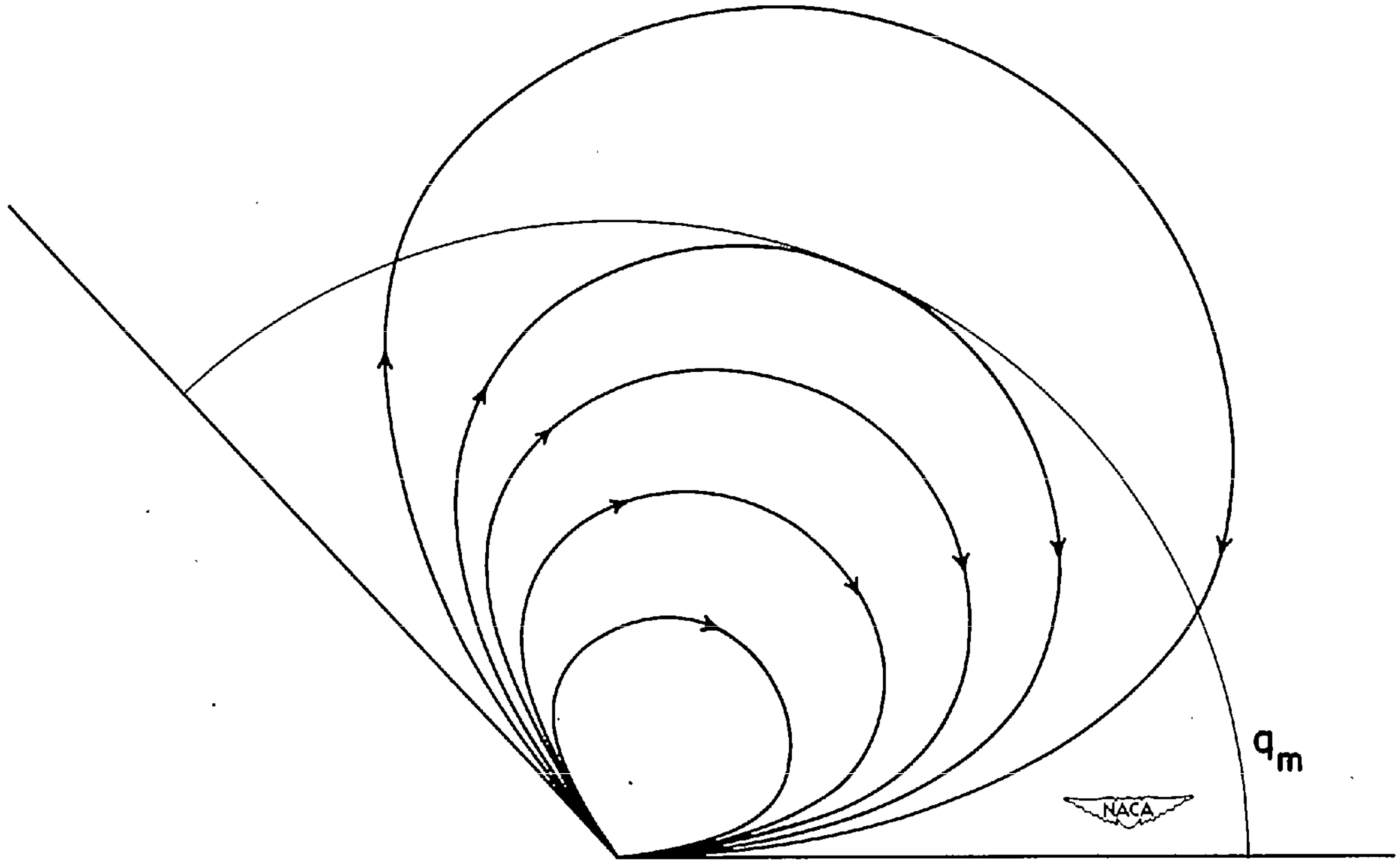

(a) Hodograph streamlines $\left(\frac{q}{q_m}\ \theta\text{-plane}\right)$ of incompressible flow.

Figure 5.- Details of flow around a corner angle of 46.8°.

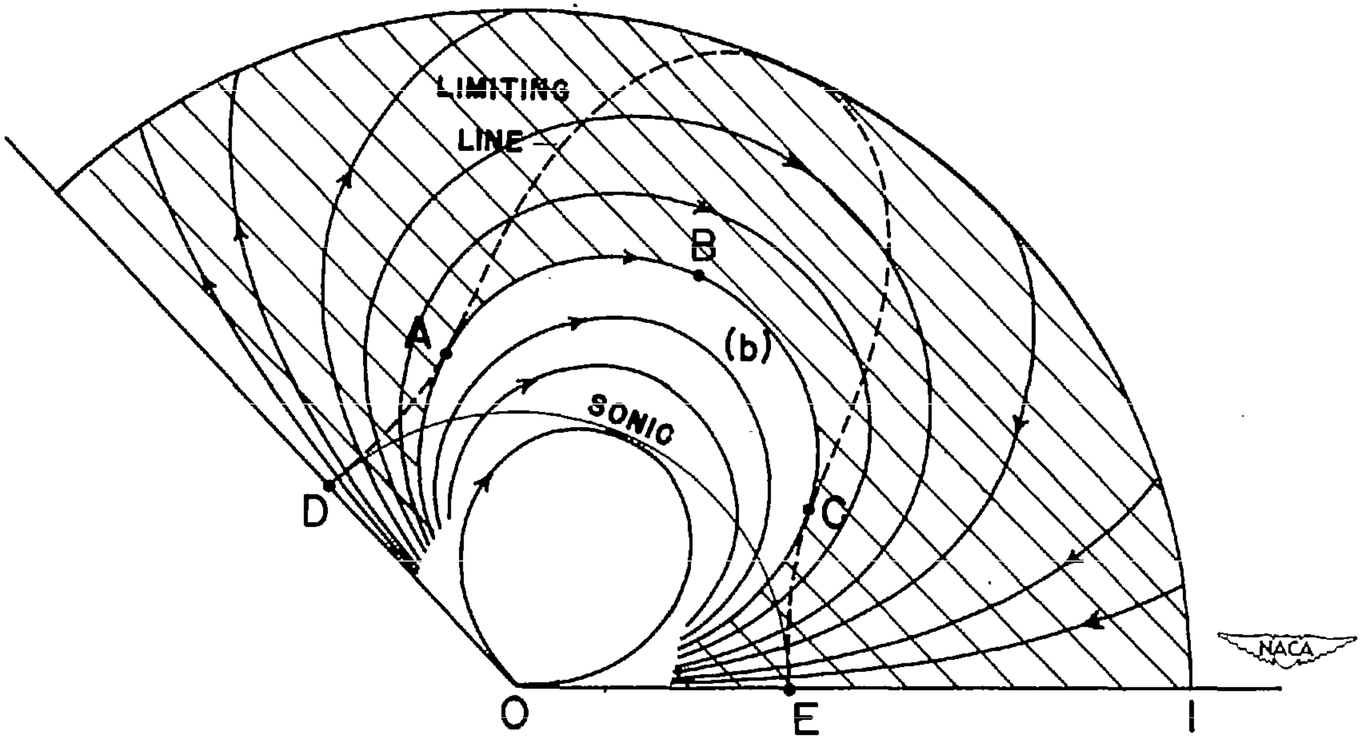

(b) Hodograph streamlines $\left(\frac{q}{q_m}\ \theta\text{-plane}\right)$ of compressible flow.

Figure 5.- Continued.

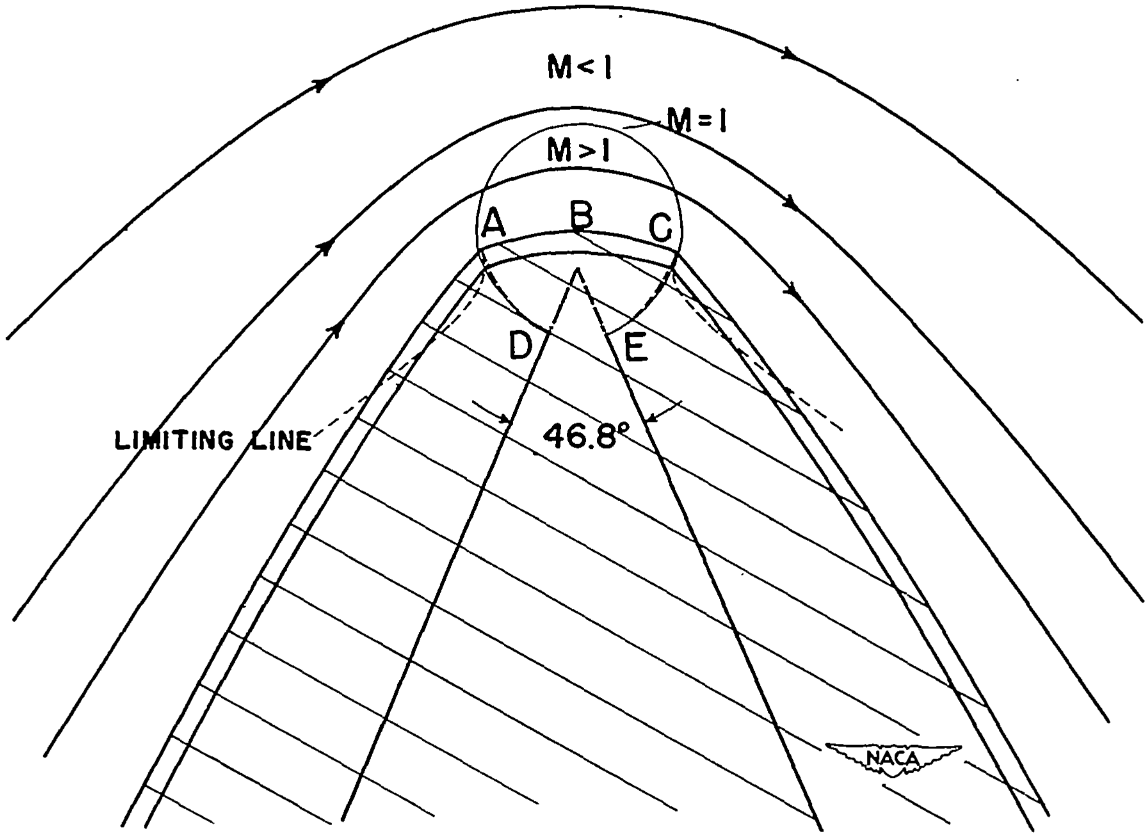

(c) Compressible flow streamlines.

Figure 5.- Continued.

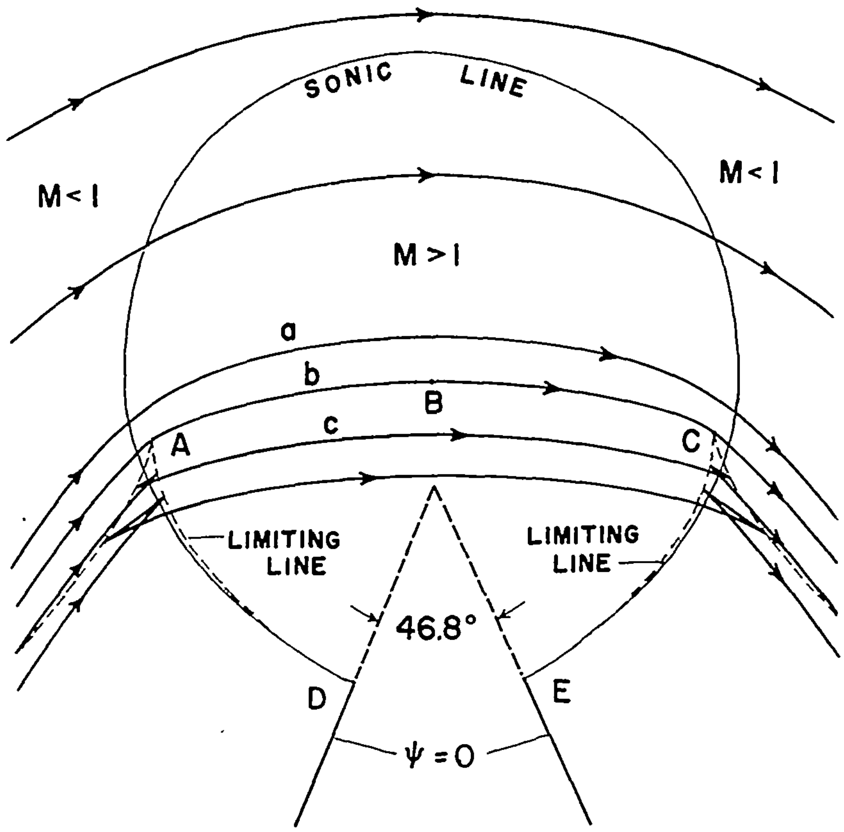

(d) Details of compressible flow.

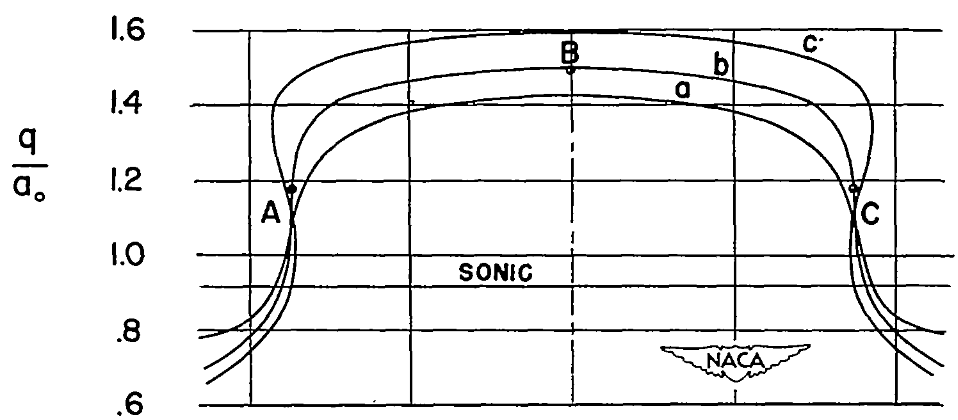

(e) Velocity distribution along some important streamlines.

Figure 5.- Concluded.

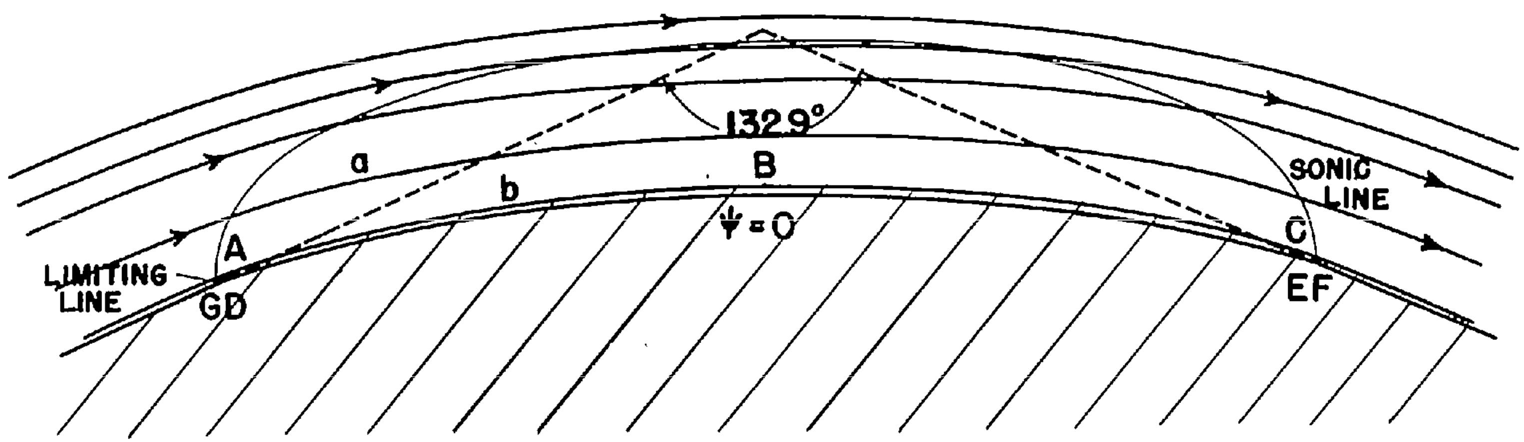

(a) Compressible flow streamlines.

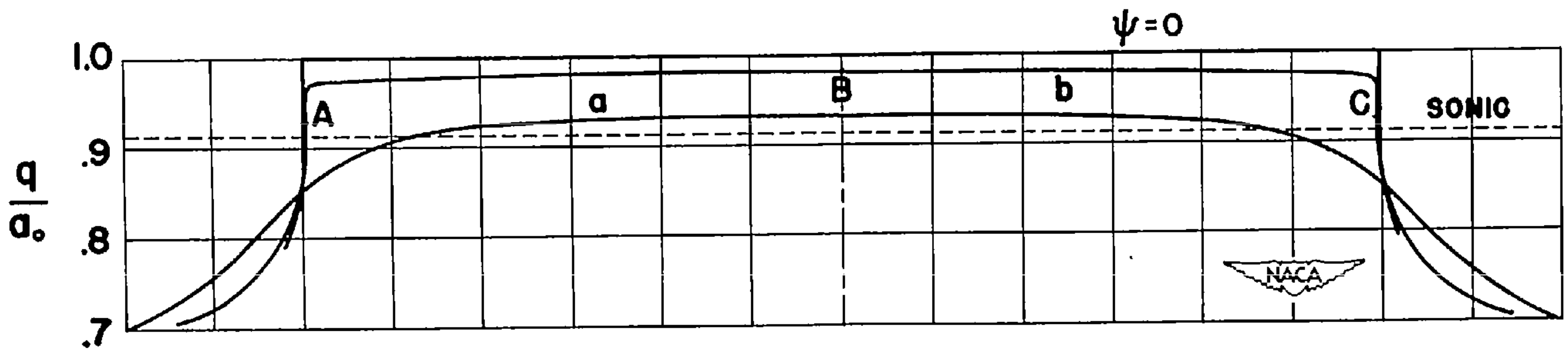

(b) Velocity distribution.

Figure 6.- Details of flow around a corner angle of 132.9°

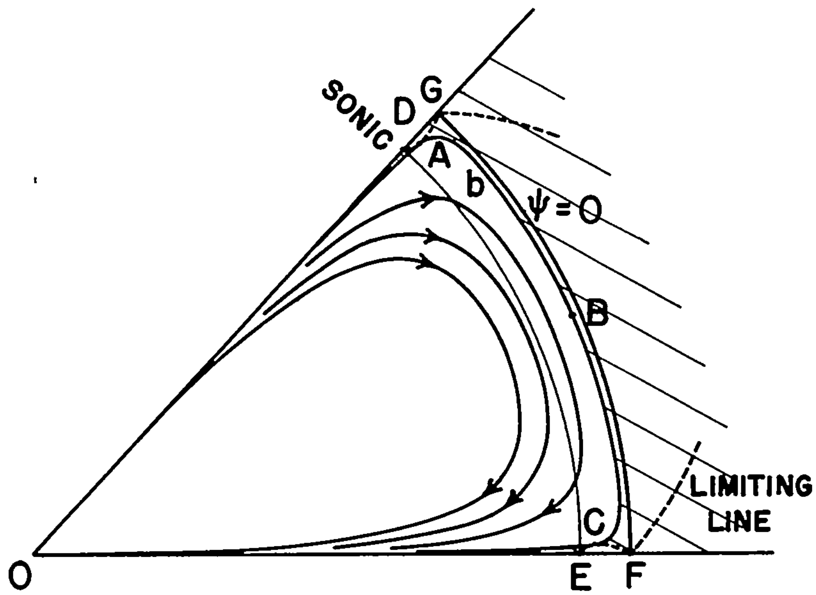

(c) Hodograph streamlines.

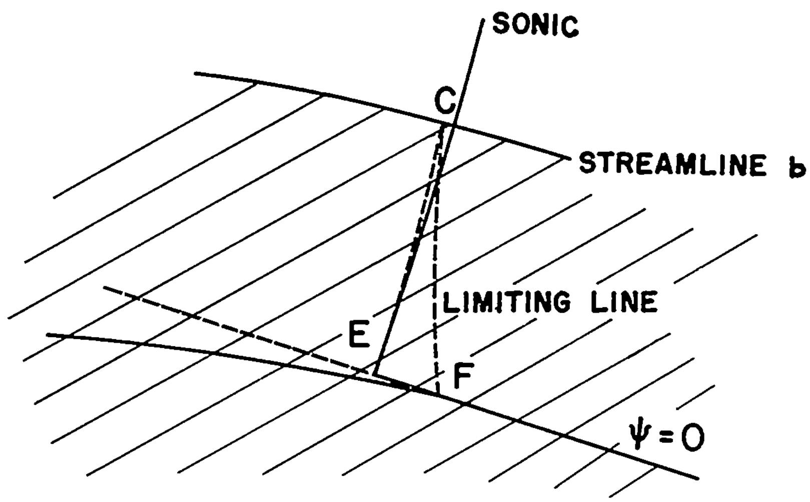

(d) Detail in physical plane.

Figure 6.- Concluded.

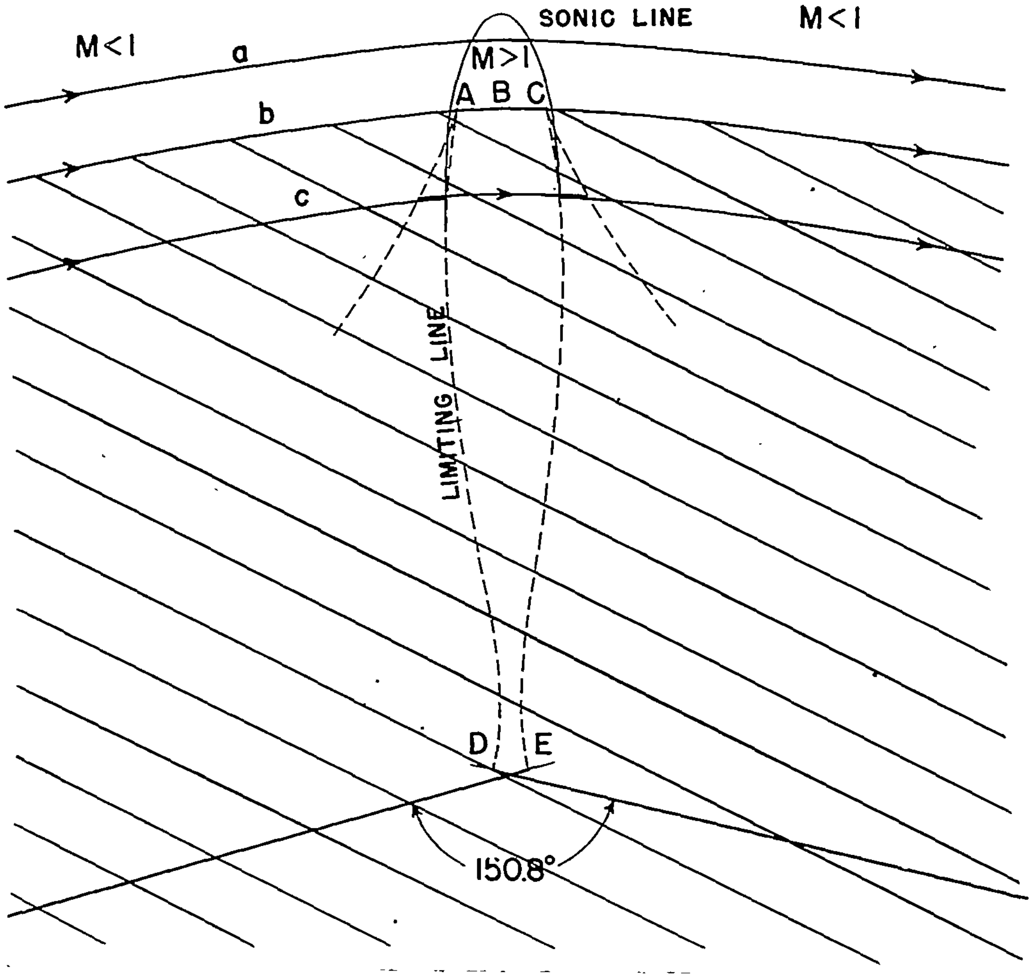

(a) Compressible flow streamlines.

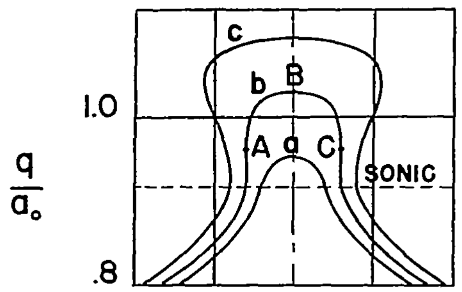

(b) Velocity distribution.

Figure 7.- Details of flow around a corner angle of 150.8°

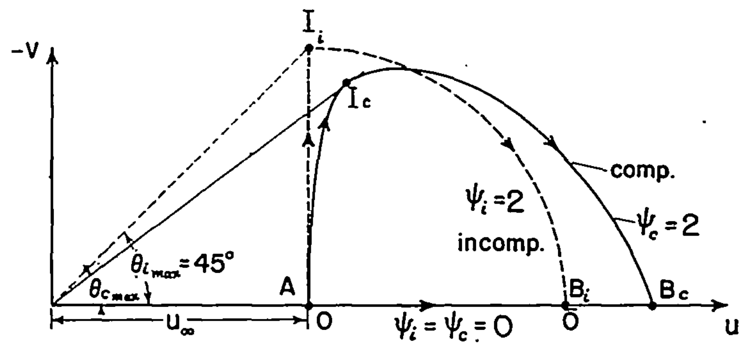

(a) Hodograph plane.

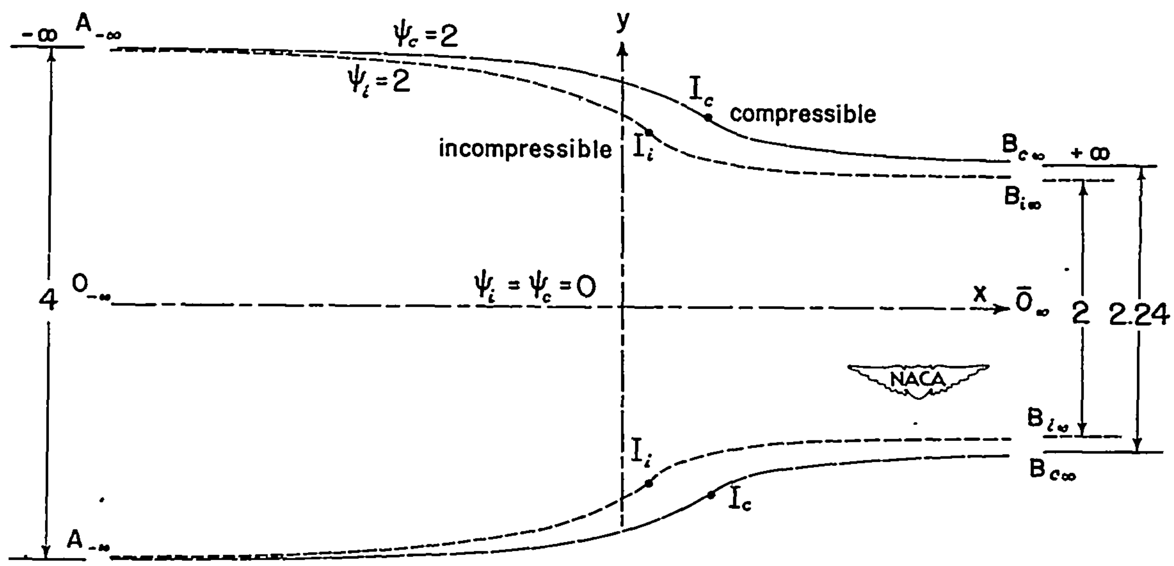

(b) Physical plane.

Figure 8.- Comparison of compressible and incompressible flow in contracting duct.

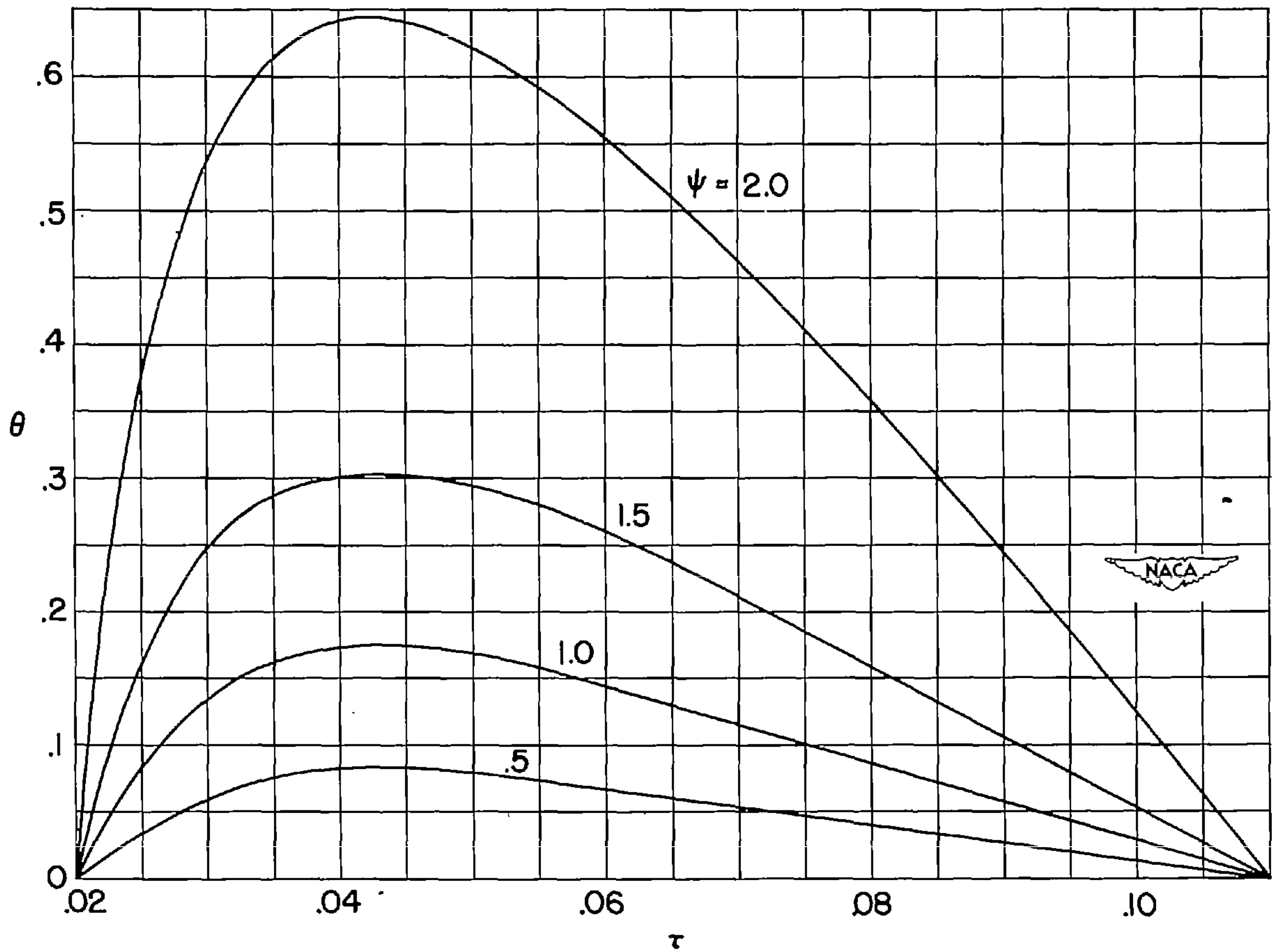

Figure 9.- Streamlines in $\tau\theta$-plane.

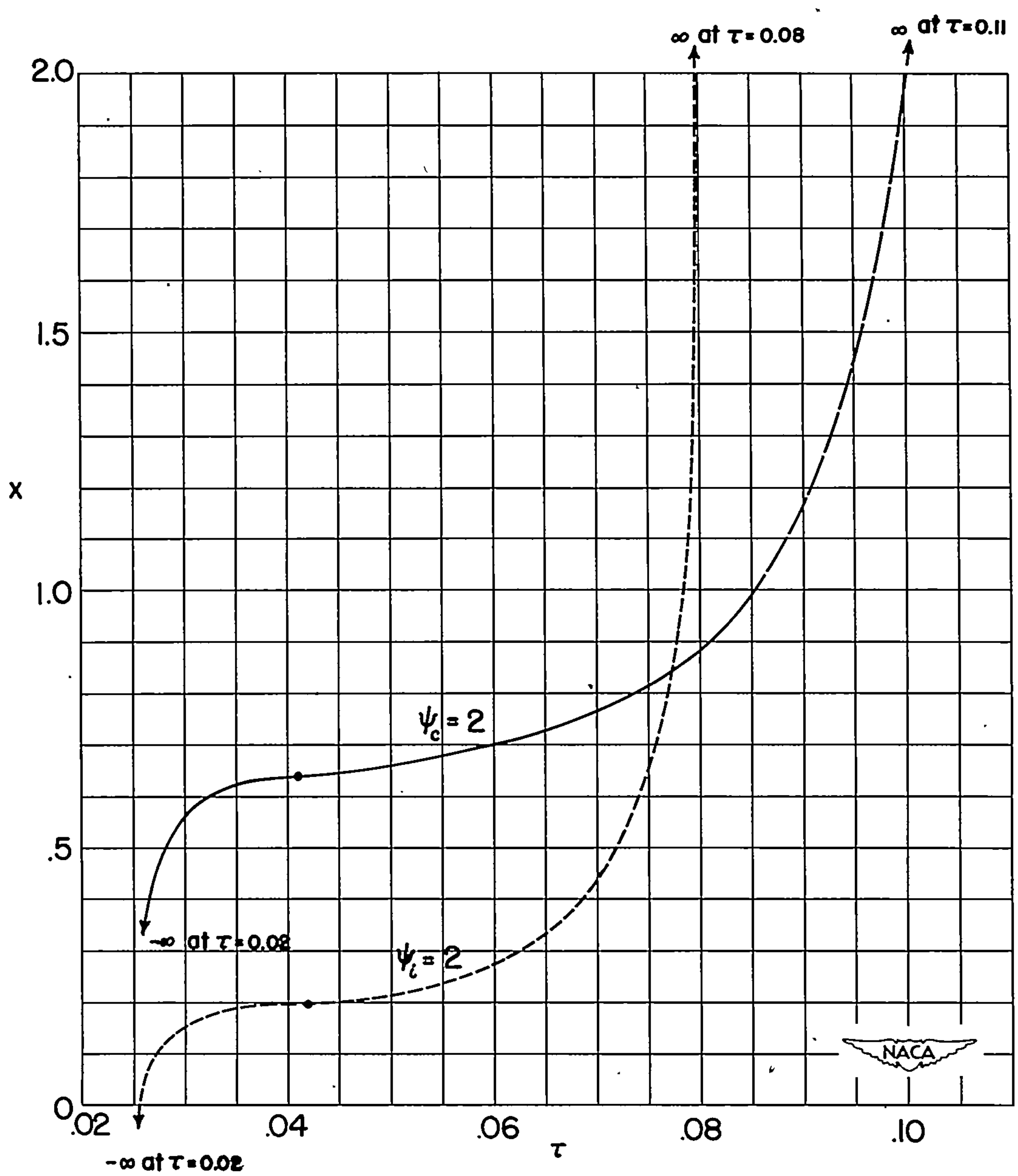

(a) x-coordinates of boundaries.

Figure 10.- Position of boundary streamlines.

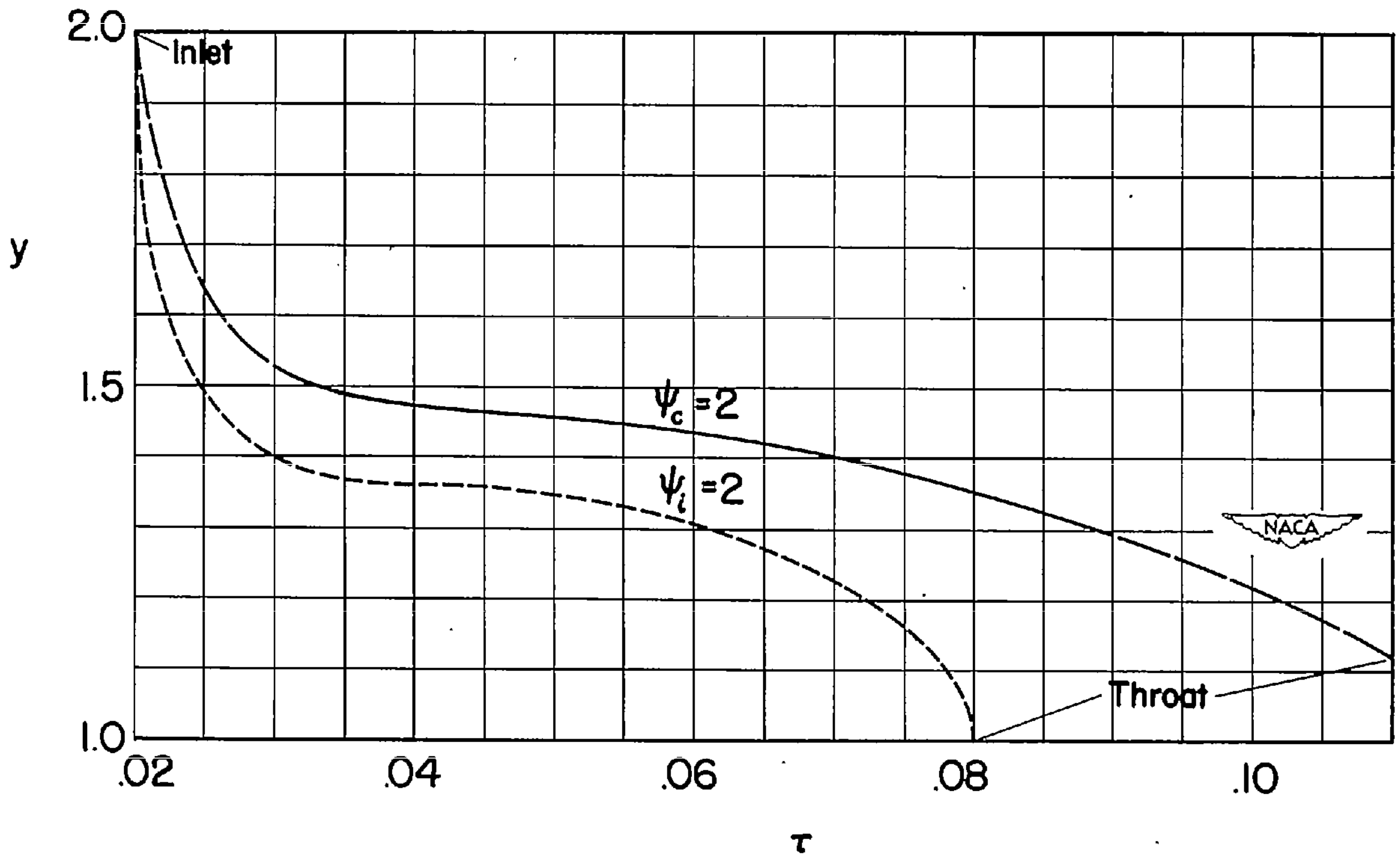

(b) y-coordinates of boundaries.

Figure 10.- Concluded.

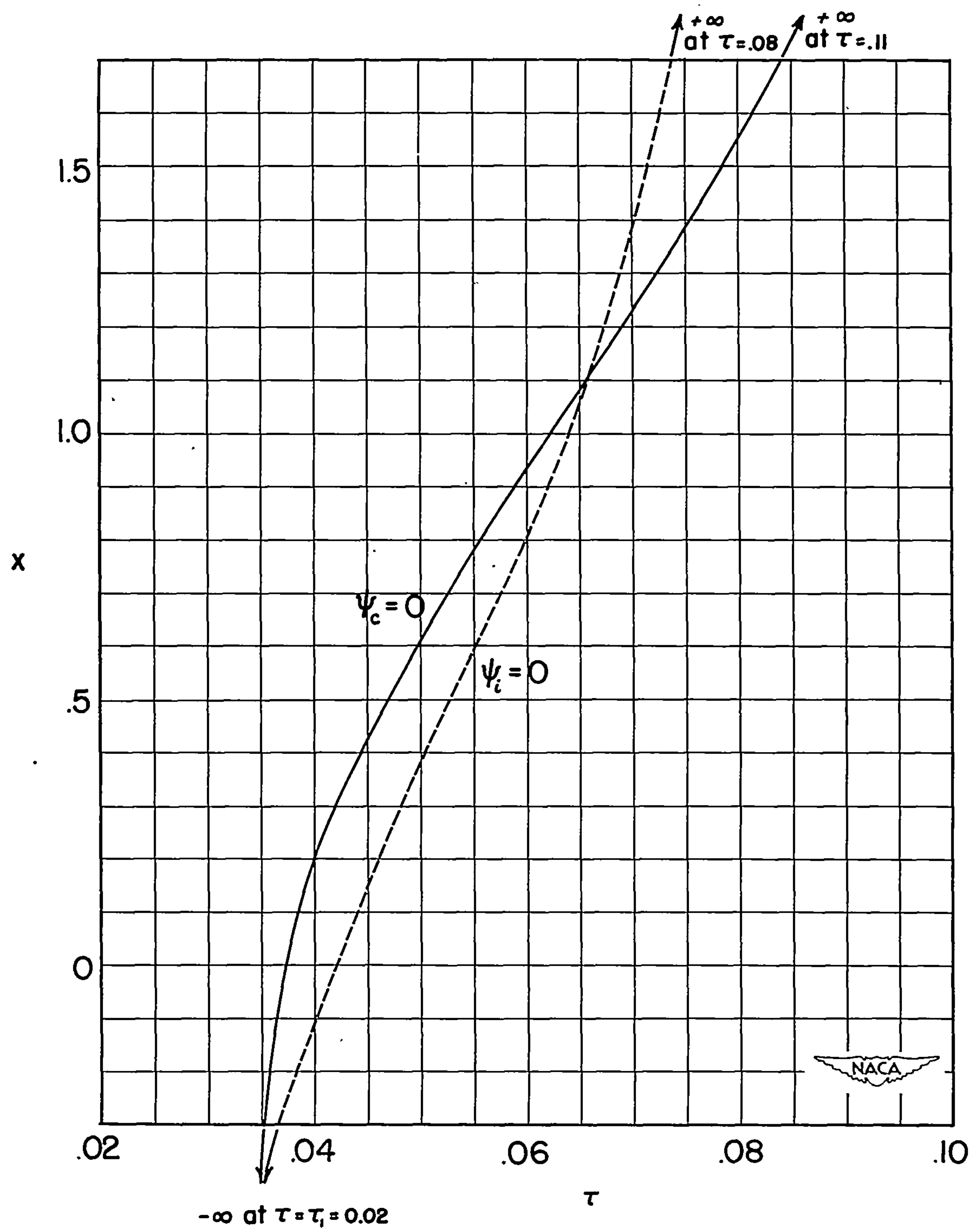

Figure 11.- x-coordinates of center streamlines.

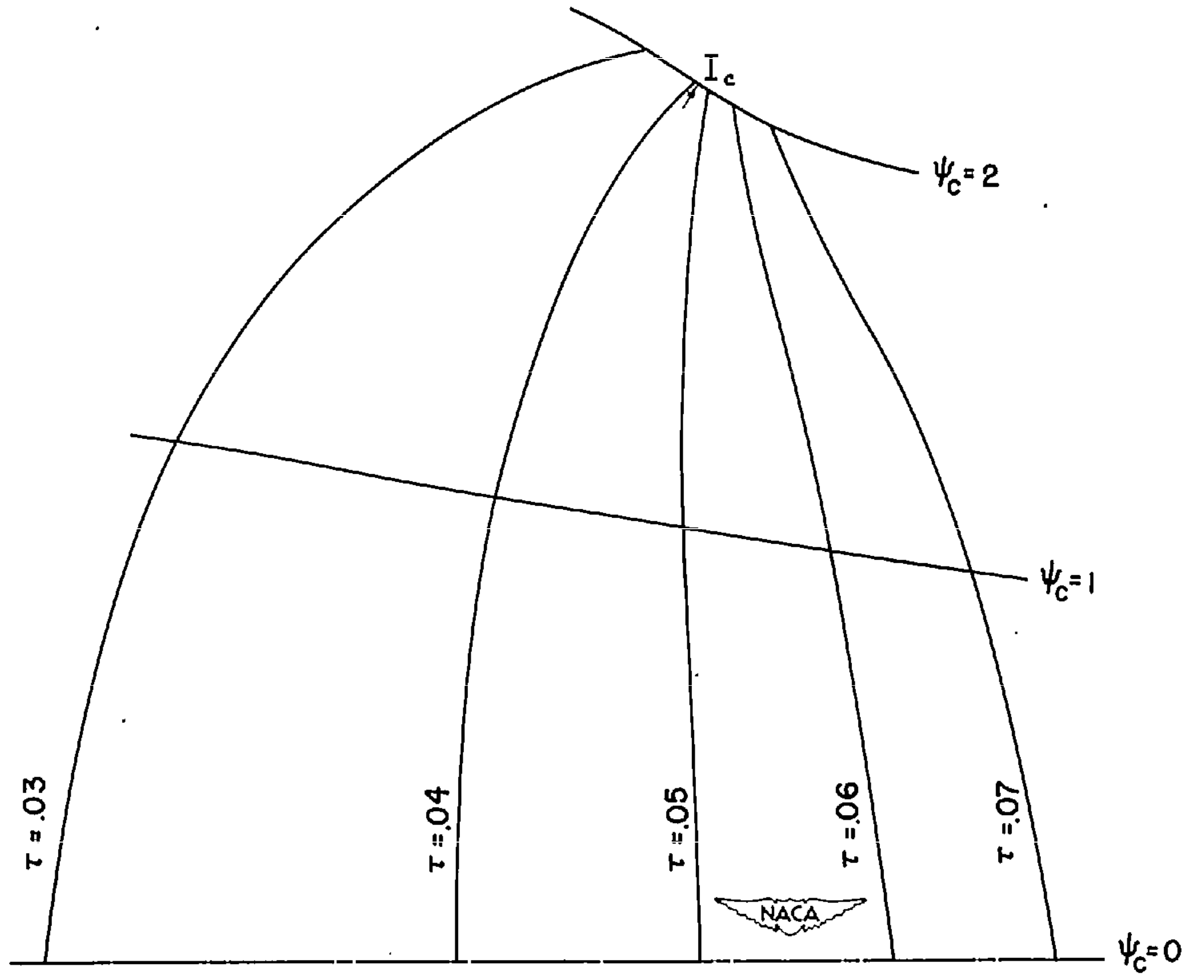

Figure 12.- Detailed compressible flow near inflection point.

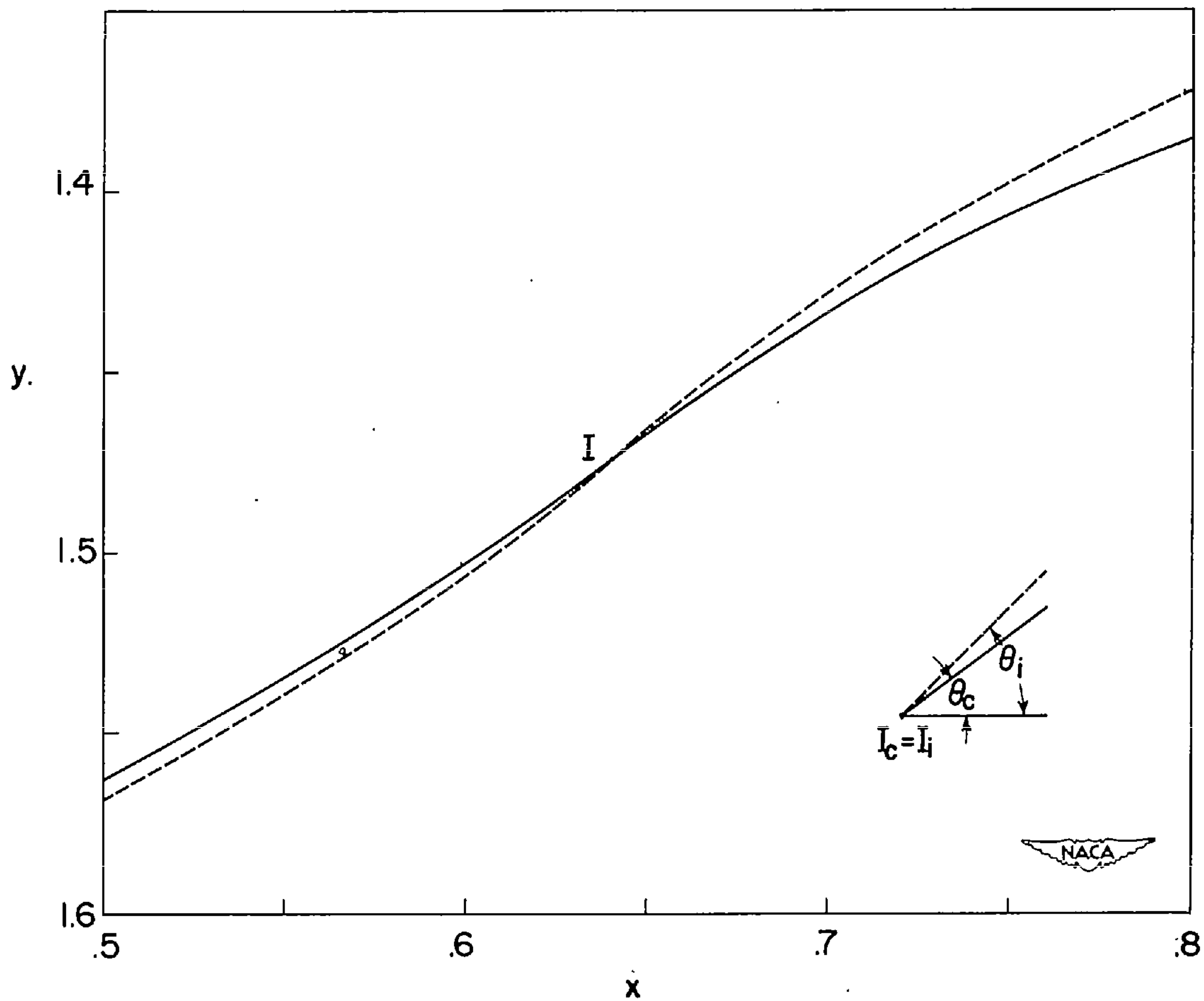

Figure 13.- Comparison of boundaries near inflection point I.

NACA-Langley - 9-1-54 - 120